IWF

ANNUAL REPORT 2003

SPACE RESEARCH INSTITUTE GRAZ
AUSTRIAN ACADEMY OF SCIENCES

ANNUAL REPORT 2003

SPACE RESEARCH INSTITUTE GRAZ
AUSTRIAN ACADEMY OF SCIENCES

Institut für Weltraumforschung
Österreichische Akademie der Wissenschaften
Schmiedlstraße 6
8042 Graz, Austria
Tel.: +43 316 4120-400
Fax: +43 316 4120-490
pr.iwf@oeaw.ac.at
www.iwf.oeaw.ac.at

Cover Image:

Rosetta will be the first spacecraft to orbit a comet's nucleus (see p. 32, Credits: ESA/AOES Medialab).

Table of Contents

1 Introduction

The Space Research Institute (Institut für Weltraumforschung, IWF) of the Austrian Academy of Sciences (Österreichische Akademie der Wissenschaften, ÖAW) understands itself as a focus of Austrian space activities. It cooperates closely with space agencies all over the world, with the academic universities located in Graz, with the Austrian Space Agency (ASA), and with numerous other national and international institutions. A particularly intense cooperation exists with the European Space Agency (ESA). IWF participates in various interplanetary missions as well as in missions dedicated to the exploration of our own planet Earth and its neighborhood. In particular:

- *Cassini/Huygens* is currently on the way to Saturn and its satellite system.
- *Cluster*, the first four-spacecraft mission ever flown, is exploring the space-time structure of the terrestrial magnetic field and the magnetospheric plasma in unprecedented detail.
- *Envisat's* radar altimeter will be calibrated by a transponder system, owned by IWF, at a cross-over site on the Greek island Gavdos.

Fig. 1.1: Artist's impression of Mars Express approaching Mars.

Fig. 1.2: Launch of the first Double Star satellite.

- After its arrival at Mars in December 2003 *Mars Express* will search for the existence of subsurface water on Mars by an onboard radar system (Fig. 1.1).
- *Double Star*, the first European-Chinese space mission cooperation, will support the *Cluster* mission. The equatorial satellite was launched in December 2003 (Fig. 1.2), the polar satellite will be launched in June 2004.
- *Rosetta* will investigate the coma and the nucleus of comet 67P/Churyumov-Gerasimenko. For the first time a soft landing on a cometary nucleus will be tried. The launch is planned for February 2004.
- *Venus Express* will investigate the atmosphere and ionosphere of the Earth's nearest planetary neighbor, Venus.

- *COROT* will search for extra-solar planets and analyze the oscillation modes of stars.
- *GOCE* will determine with high accuracy and resolution the structure of the terrestrial gravitational field to foster a better understanding of the Earth's interior, global ocean circulation, heat transport mechanisms, and contribute to a worldwide unification of regional height systems.
- *THEMIS* will fly five identical microsatellites to give the ultimate answer to the long-standing question about the causal relationships in the chain of processes called magnetospheric substorm and to the origin of auroral phenomena.
- *BepiColombo* will investigate in detail the innermost planet Mercury, using two orbiters: one with instruments specialized for magnetospheric studies and the other for remote sensing of the planet.

In addition, IWF performs a wealth of theoretical investigations, data analysis, and laboratory experiments on gravitational and magnetic fields, on atmospheres and on surface properties of solar system bodies. Moreover, at Lustbühel Observatory in Graz one of the most accurate laser ranging stations of the world is operated. Its data are used to determine the orbits of more than 30 satellites. Also located at Lustbühel Observatory is a system of antennas used to monitor the radio emissions of Jupiter and the Sun. Finally, a network of nine permanent GPS stations is operated by IWF in order to monitor geodynamical movements in Austria and its vicinity.

IWF is located in an attractive building, the "Forschungszentrum Graz" (Research Center Graz) of ÖAW. Its managing director, Prof. Dr. Hans Sünkel, is at the same time rector of the Graz University of Technology.

IWF is structured into three departments:

- Experimental Space Research
  (Head: Prof. Dr. Wolfgang Baumjohann)
- Extraterrestrial Physics
  (Head: Prof. Dr. Helmut O. Rucker)
- Satellite Geodesy
  (Head: Prof. Dr. Hans Sünkel)

The bulk of financial support for our research comes from ÖAW. Substantial support is also provided by other national institutions, the Austrian Space Agency (ASA), the State of Styria, the Austrian Science Fund (Fonds zur Förderung der wissenschaftlichen Forschung, FWF), the Austrian Council for Research and Technology Development (Rat für Forschung und Technologieentwicklung, RFTE), and by the Austrian Academic Exchange Service (Österreichischer Akademischer Austauschdienst, ÖAD) and its partner institutions in other countries. Last but not least, European Institutions like the European Space Agency (under the PRODEX and GOCE Programs) and the European Union (under the INTAS and 5th Framework Programs) contribute substantially.

2 Solid Earth

How is the actual status of the surface of the Earth and its near vicinity? Can permanent monitoring lead to a possible prediction of future global changes and, if yes, how?

Questions for our "blue planet" which find the answer in a nearly unlimited bulk of data provided by satellites, equipped with special sensors for different tasks. They outline a global image of our planet with, up to now, unknown resolution, which allows for the investigation of detailed structures. The task remains how to de-correlate individual phenomena and to pick out the specific elements which are required for the understanding of the basic physical processes.

For example, the precise knowledge of the Earth's gravity field and its temporal changes contributes to the detection of the mechanisms leading to the building of the Earth's crust, the evolution of the green house effect and the flow of ocean currents. The repeated determination of precise station coordinates via GPS and Satellite Laser Ranging leads to the definition of a temporally changing velocity field, allowing the investigation of the underlying driving forces and the energy transport in the Earth's interior.

2.1 Gravity Field

Gravitation, the universal force of attraction exists between all particles with mass in the universe. The gravity field of the Earth is the direct response to its interior mass density distribution and the centrifugal force caused by its rotation. The inhomogeneous distribution of mass in the Earth's interior and the ruggedness of the topography are the main causes for irregularities in a global gravity field map of the Earth.

The irregular gravity field of the Earth shapes a virtual surface at mean sea level called the geoid. This is the surface of equal gravitational potential of a hypothetical ocean at rest and it serves as the classical reference for all topographical features. The accuracy of its determination is important for surveying and geodesy, e.g. for the unification of height systems, furthermore for studying physical and dynamical processes in the Earth's interior, to model large scale ocean circulation, and to monitor ice motion and sea-level changes, to name its most important applications.

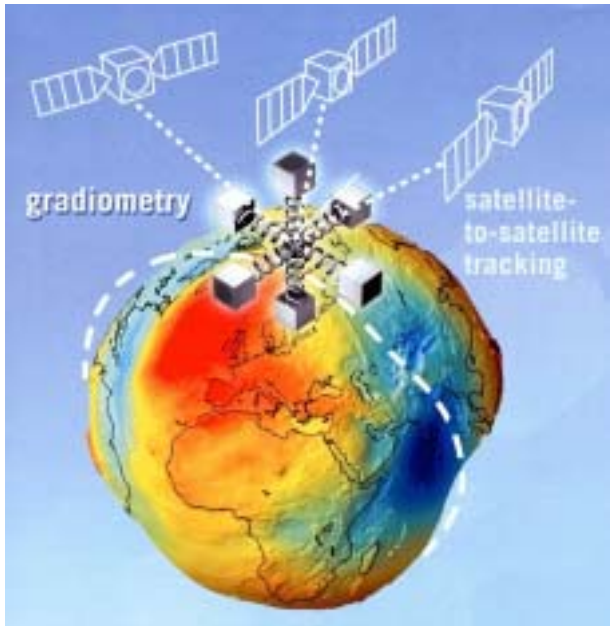

Fig. 2.1: Determination of the geoid shape by means of the sensor fusion concept of ESA's GOCE satellite mission.

GOCE Mission

The Gravity Field and Steady-State Ocean Circulation Explorer *(GOCE*, Fig. 2.1) satellite mission is a dedicated gravity field mission,

which was selected in 1999 as the first Earth Explorer Core mission as part of ESA's Living Planet Programme. This mission, to be launched in 2006, aims at measuring the Earth's global gravity field and modelling its associated geoid with extremely high accuracy and resolution (Fig. 2.2).

Fig. 2.2: Artist's impression of the GOCE satellite in orbit.

For this purpose *GOCE* employs for the first time a sensor fusion concept, using a combination of the principle of satellite gravity gradiometry (SGG) and satellite-to-satellite tracking (SST) relative to GPS satellites. The concept of SST, developed back in the 1960's, is based upon tracking the orbit differences between satellites that experience different gravitational accelerations at different locations, whereas the SGG measurement principle is based upon analyzing the difference in gravitational acceleration of proof masses within one satellite. The two measurement principles complement each other perfectly, since the ultra-precise gradiometer device is used to measure the high-resolution features of the gravity field, whereas the large-scale features are provided via the satellite's orbital SST information. The *GOCE* gravity field mission is complementary to the currently flown gravity missions *CHAMP* and *GRACE* and it will deliver a high-resolution gravity field model with a geoid accuracy of about 1 cm at a new range of spatial scales in the order of 100 km half wavelength.

This high-accuracy and high-resolution global gravity information will make a deep impact on many branches of Earth Sciences. It will be applied in geophysics to improve the modelling of the Earth's interior. In combination with satellite radar altimetry, it will revolutionize the accuracy of the models of global ocean circulation, which is responsible for about 70% of the global heat and energy transport, and thus plays a crucial role in climate regulation. Last but not least, also geodesy will highly benefit from an improved global gravity model, which will provide a high-accuracy global height reference system, and thus will allow levelling by the use of global positioning systems (GPS, *Galileo)*. Additionally, it will improve the prediction of satellite orbits, and will contribute to many applications in positioning and navigation.

GOCE DAPC Graz

The scientific objective of the project "GOCE Data Archiving and Processing Center (DAPC) Graz" is the design and installation of an operational software prototype for the *GOCE* data processing, with the goal of deriving an optimum gravity field solution from SST and SGG observations (Fig. 2.3). This is complemented by a database and archiving system for data retrieval and long-term storage.

The project work has been performed by a joint effort of the Graz *GOCE* Team, which is a close co-operation of IWF with the Institute of Geodesy of the Graz University of Technology.

Key items that have been addressed during the first project phase are:

- Design of the database prototype
- Definition of *GOCE* standards
- Pre-Processing of SST and SGG data
- Gravity field solution: Including the Quick-

Look solution approach, the core solvers for SGG and SST, and their optimal combination

- Software Validation Plan

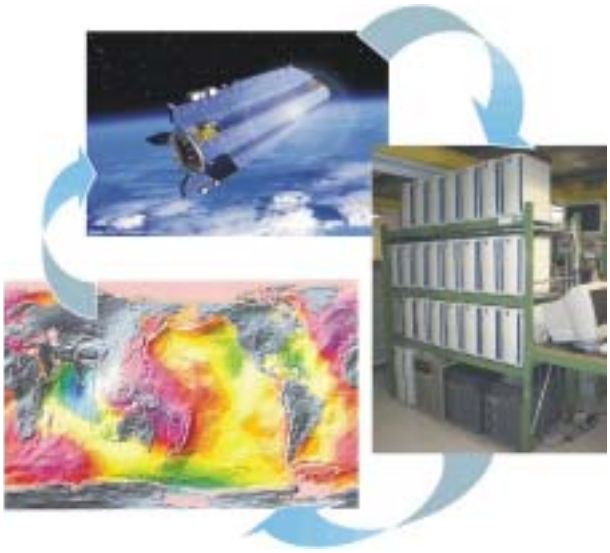

Fig. 2.3: GOCE processing circle from measurement data to scientific data processing to a model of the gravity field of the Earth.

In the following a short overview of the SST solver concept and the optimal combination approach of SST and SGG shall be given.

Energy integral: The information content of the SST data is utilized by making use of precise *GOCE* orbits expressed in terms of position and velocity information including quality description. In contrast to the standard method for the exploitation of the orbit information, i.e. the integration of the orbit perturbations and variational equations, the principle of energy conservation is applied as the baseline strategy. Favorable features of this approach are a strictly linear observation model, as well as the fact that gravity functionals are processed. The feasibility of this method is underpinned by several studies, showing that recent POD (precise orbit determination) strategies are able to deliver orbit information with sufficient accuracy. The concept has also been sufficiently demonstrated with real data of the *CHAMP* mission.

The energy integral is based on the law of energy conservation: $E_{kin} + E_{pot} = \text{const}$. This formulation only holds, if only conservative forces (i.e. the gravity field of the solid Earth) are considered. Since satellite orbits are affected by many other influences the energy conservation law has to be extended for non-conservative forces (i.e. atmospheric drag), and temporal variation effects (i.e. potential of the rotating Earth, ocean tides). Output are the spherical harmonic coefficients C_{lm}, S_{lm} of the harmonic series expansion of the Earth's gravity field, the energy constant and scaling and bias of the accelerometer data.

The influence of non-conservative forces and temporal variations have to be investigated in detail in order to remove their influence on the energy balance. Different approaches for modeling these data, and application to real *CHAMP* accelerometer data (measuring the influences of non-conservative forces) are under investigation.

Fig. 2.4 and Fig. 2.5 show the degree error RMS and the residual energy when applying *CHAMP* accelerometer data to the energy integral using a drift parameter, polynomial of higher degree and tides.

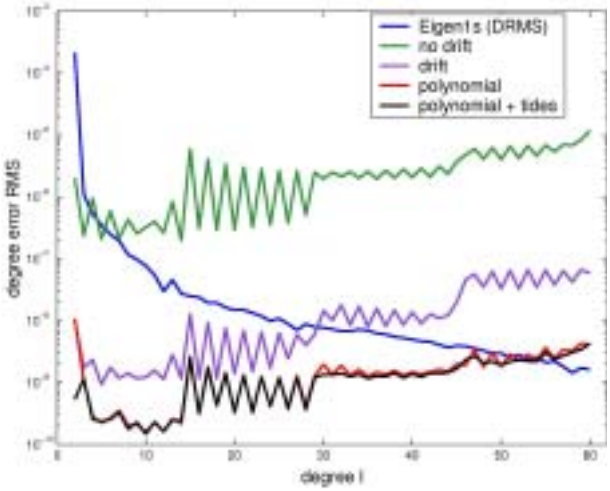

Fig. 2.4: Degree error RMS (drift, polynomial approximation and tides).

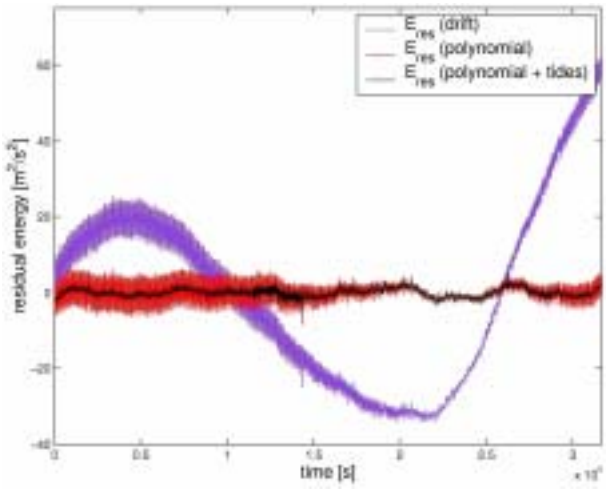

Fig. 2.5: Residual energy (drift, polynomial approximation and tides).

Regularization: In order to fully exploit the information content of the combined *GOCE* sensor system, the mathematical models for SGG and SST data are combined to the overall mathematical model by means of superposition of the normal equation systems. The ill-posedness of the normal equations due to the polar gaps (as a consequence of the sun-synchronous orbit with an inclination of 96.6° the polar regions are not covered with measurements) and the downward continuation have to be managed by optimized regularization techniques.

A second effect of regularization is the suppression of high-frequency noise. Further, weighting parameters have to be applied to the individual normal equation systems, resulting in an optimum relative weighting of the data types of SGG and SST, and thus in optimum gravity parameter estimates. Several methods for regularization as well as for optimum weighting are analyzed with respect to the special requirements of the *GOCE* mission. To compare the performance of the investigated methods, several closed-loop simulations have been performed.

Investigations of widely-used regularization methods have emphasized that they cannot alleviate the ill-posedness of the system in a satisfactory manner. Minimizing the oscillations at the polar regions leads to an unintended damping of the high-frequencies of the gravity field in a global scale. This is why the investigated standard techniques do not adequately treat the polar gap problem.

In the framework of our research a regularization method has been developed that stabilizes the model exclusively at those regions, where no measurements are given. The so-called Spherical Cap Regularization Approach (SCRA) addresses directly the polar gap problem and its application in closed-loop simulations showed extraordinary results (Fig. 2.6). Since sun-synchronous orbits are a problem in global data recovery in general, the developed method can also be used in disciplines other than gravity field determination.

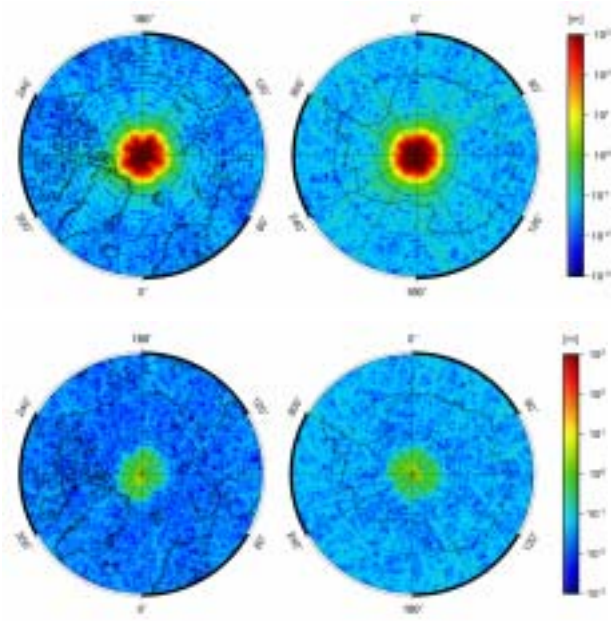

Fig. 2.6: Geoid error at the North and the South pole if no regularization was applied (top) and if SCRA was applied (bottom).

2.2 Geodynamics & Meteorology

Disaster prevention is one of the most important challenges for preservation of our short lifetime and of property. Life is dangerous by definition – we cannot outwit the laws of nature! And if we try it we see immediately that we could not realize the consequences of our actions. Disaster prediction relies on experi-

ence, which in our days is not only based on history but on well certified data sets. The more accurate these sets are the better short-wave and even secular processes can be monitored. Precise coordinates are the pre-requisite for geodynamical investigations, real-time products for fast dynamic changes as e.g. changes in the atmosphere. Besides, we have also to include the monitoring of sea-surfaces as their status is intimately connected with geodynamical events (e.g. Tsunamis) and climate changes and gives indirect conclusions about the net-effects of these influences. We cannot cover the whole field but we try to give valuable contributions in the global context.

Reference Frame

We operate a data and analysis center which stores all data of the Austrian as well as of *CERGOP-2* GPS-reference stations and computes the coordinates of a selected set of European stations on a regular basis (daily/weekly). The results are included in the European weekly solution, which determines the actual, timely varying, reference system of Europe. In addition, we are responsible for monitoring sudden changes of coordinates in southeast Europe (down to Israel), which may indicate a response to geodynamical activities (Fig. 2.7), the part of Europe showing the most seismic activities during the last decades. This perfectly fits into our program of monitoring crust movements.

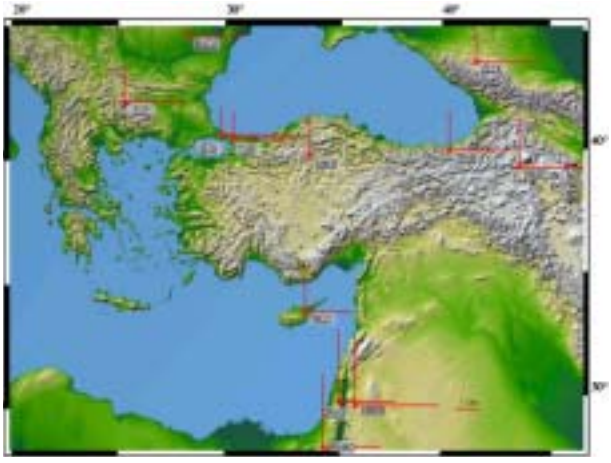

Fig. 2.7: EUREF stations controlled by IWF.

CERGOP-2/Environment

The aim of the project *CERGOP-2/Environment* with 14 partners from 13 countries of the Central European Initiative is the establishment, maintenance and monitoring of a reference frame for geodynamical research covering about 15% of the European area. Local investigations in seismic active regions will supplement the overall objectives. The final output will be a timely varying velocity field, which gives the basis for geodynamical investigations in this region, i.e. allocation of the underlying forces and the energy transfer leading to earthquakes. Fig. 2.8 shows the present distribution of GPS-monitoring CEGRN stations.

Fig. 2.8: The geodynamic reference frame CEGRN (red square: permanent stations, blue square: proposed permanent stations, red triangle: accepted epoch stations, blue triangle: proposed epoch stations).

This project is also highly correlated with the planned INTERREG initiative for monitoring the complete alpine region. It was approved and started in April 2003. First results are: the performance of the CEGRN'2003 campaign in June 2003 and the establishment of a seamless data bank in Graz. Another work package aims at the construction of a modular design of a permanent GPS-station, which will be

installed in most of the partner countries. Its completion is expected during the next three months.

GAVDOS

GAVDOS aims at the establishment of a European radar altimeter calibration and sea-level monitoring site for *Jason*, *Envisat* and *EUROGLOSS* on the Greek island of Gavdos. The project involves 9 partners with the Technical University of Crete being the coordinator. IWF is responsible for the determination of the radial and along track component of satellite orbits by the use of a satellite transponder. This gives among other observation techniques employed in the project an independent method for altimeter calibration and orbit determination.

In preparation of moving the transponder to Gavdos some test measurements in Austria had to be performed. Deployments in Güssing, Gaberl, St. Lorenzen and Lassnitzhöhe verified that the transponder is working properly.

In order to simulate the Greek measurement scenario from the geographical point of view, i.e. to locate the transponder close to the sea, we decided to deploy the equipment at some suitable sites at the Adriatic Sea. Measurements in Cres and Umag (CRO) showed that the transponder is able to influence the mode of operation of the satellite radar altimeter.

As the transponder is intended to work permanently and unattended on the island of Gavdos, many precautions had to be taken. A suitable housing was built in order to protect the equipment from the sometimes very rough weather conditions (Fig. 2.9). On the other hand proper materials had to be chosen in order to minimize the influence on the measurement signal.

End of September the transponder was finally shipped to Greece and successfully deployed on Gavdos beneath the crossover point of the *Jason-1* spacecraft. The transponder was provided with an external power supply and programmed for the upcoming satellite passes covering the next six months.

Fig. 2.9: Transponder within its housing mounted on a concrete base on Gavdos island.

First measurements have been made successfully (Fig. 2.10) and extensive analyzes on the upcoming data have now to be carried out in order to deduce the absolute ranges to the spacecraft. Due to the very sophisticated and new concepts of the *Jason-1* altimeter *(Poseidon-2)* a lot of further software developments of the current *ERS-1/2* analysis software have to be made.

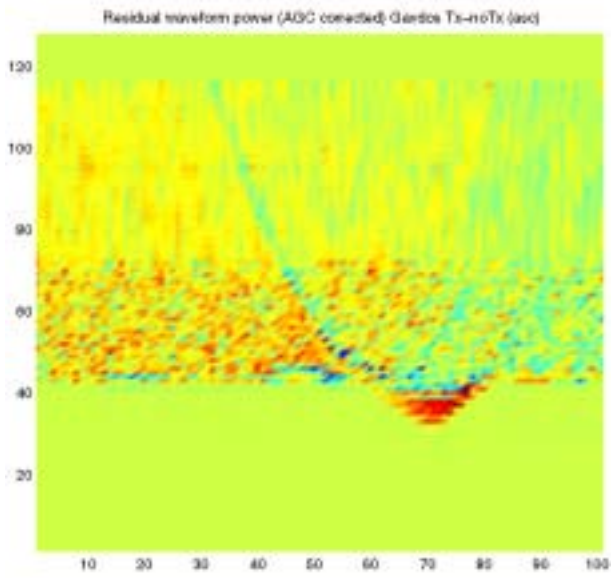

Fig. 2.10: Transponder response from a satellite pass at Gavdos (x-axis: flightpath, y-axis: signal power).

ISDR

The program *ISDR* (International Strategy of Disaster Reduction) is the successor of the UN Project IDNDR (International Decade of Natural Disaster Reduction, 1990–2000) and gives us the required additional funding for establishing and maintaining a reference network in Austria for monitoring local crustal movements. The complete bulk of stations (more than 20 at the moment, see Fig. 2.11) is now used for all kinds of research like crust dynamics monitoring, near real time data production (water vapor) and commercial use. During the current year we could only maintain the present network; computer problems affecting the data communication led to increasing work outside of Graz. A new receiver was bought to be operated at Zettersfeld near Lienz and the case-studies in Innsbruck and Reisseck were continued. The planned remonitoring of Slovenian sites (after the earthquake 1998) is now included in *CERGOP-2/Environment*.

Fig. 2.11: The Austrian permanent array of GPS monitoring stations.

COST-716

Four years after its start, COST-716, a cooperation between geodesists and meteorologists for numerical weather prediction and climate research, was terminated with a final workshop at KNMI in De Bilt, Netherlands. More-accurate weather forecasting requires a dense European network of GPS receivers and the use of the very latest observations and processing techniques for estimating the water vapor by signal delay analysis. Four working groups revealed the present status (Graz), a benchmark campaign (Delft), data assimilation (Delft), and the step to an operable network (London). The Austrian permanent GPS-network delivers hourly data for that purpose. A work package of *CERGOP-2/Environment* is dedicated to study the influences of troposphere to GPS height determination or, equivalently, to extract the delay information with pre-supposed fixed height for meteorological applications. The use of zenith delays for weather forecasting will depend on the accuracy of GPS-measurements (plus *GLONASS* and later *Galileo)* and the near real time aspect for data delivery (less than 1 hour). Doubtless GPS delay measurements are significant for climate research.

The final project report is in preparation. More information is available at the web page of the UK Met Office (www.metoffice.gov.uk) and at www.oso.chalmers.se/geo/cost716.html.

2.3 Satellite Laser Ranging

Ongoing Measurements

In 2003 we were able to break all our previous internal high scores: Until October, we have already tracked successfully more than 6500 passes, more than in any full year before (Fig. 2.12). This increase of data yield was also due to the excellent weather conditions; usually we get more than 95% of all possible passes, if the weather is okay.

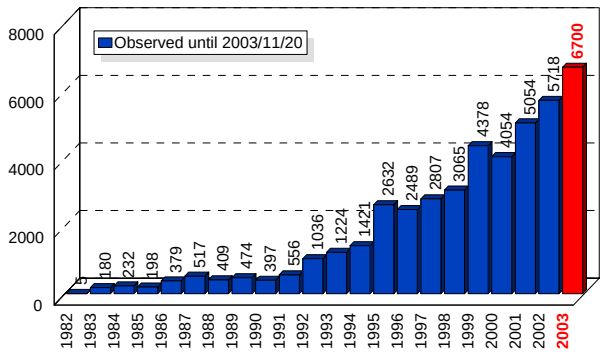

Fig. 2.12: Graz SLR Tracking per year.

We also could keep our very high level of stability and reliability: In all relevant data checks, the Graz SLR data is among the first stations worldwide. For satellites with low satellite signature (*ERS-2*, *Envisat*, *Jason-1*, *GRACE-A/-B* etc.) as well as for standard calibrations, we get a minimum RMS of about 3-4 mm single shot (see Fig. 2.13).

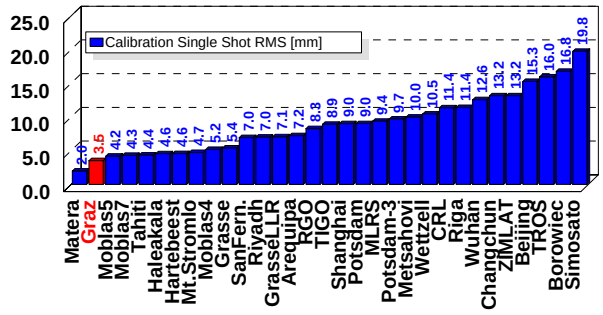

Fig. 2.13: Calibration RMS for LAGEOS.

The new kHz Laser

Since the last four years, we have worked consequently towards a completely new kHz Laser system. Every hardware upgrade, any new piece of software was implemented with the possibility of kHz ranging in view.

It started with the development and installation of the Graz Event Timing System (E.T.), continued with the development of new Range Gate Generators (RGG, RGG2), development of algorithms and electronics for laser start pulse generation (and shifting in case of coincidence with returns), upgrade of the real time computer system, and ended finally with the successful implementation of a complete new software for kHz ranging, and for handling the Megabytes of kHz ranging data (Fig. 2.14).

Since about two years, a new type of lasers is available, which is completely diode pumped (DPSSL: Diode Pumped Solid State Laser), can produce pulses with less than 10 ps pulse width at repetition rates of up to 2 kHz, and is very promising in terms of stability, maintenance etc. However, the energy per pulse is rather small (a few hundred Micro-Joules), as compared to the usual 30 to 50 Milli-Joules used in most SLR stations. However, all calculations showed that this drawback would be much more than compensated by the higher repetition rates.

The first and only company offering such a device was HighQLaser, an Austrian company. The main final specifications of our new laser are now: Nd:Vanadate, DPSSL, 10-2000 Hz repetition rate, <10 ps pulse width, 0.4 mJ/shot at 532 nm, and with a beam quality M^2<1.5.

Since October 2003 the Graz SLR station is fully operational with 2 kHz. Thus, it is the first SLR station worldwide capable of kHz operation; all other stations operate with 5 or 10 Hz.

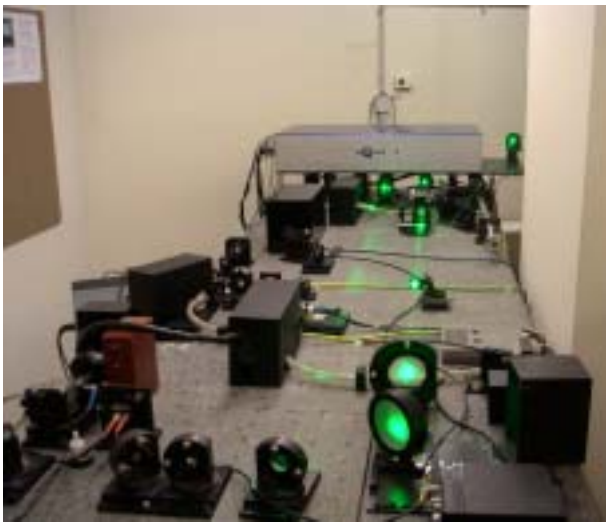

Fig. 2.14: The new kHz Laser: Small blue box in the background, on top of the old 10-Hz-Quantel Laser.

kHz Range Gate Generator: A new, substantially improved and extended version of the Range Gate Generator (RGG), as in principle described already in the 2002 report, was designed, built and implemented into the Graz SLR system. This device offers a resolution of <500 ps, allows laser repetition rates of some kHz, and is fully programmable via PC and a standard 16-bit interface. It is implemented in FPGA technology. The selected FPGA chip contains about 1 million gates, of which we use now about 20%, leaving enough space for future upgrades and add-ons. It not

only contains this new RGG2, but also produces all necessary pulses to fully control the new kHz laser, including programmable repetition rates from 10 Hz up to 2000 Hz. It also features automatical shifts of these laser firing pulses to avoid laser firing near expected return times (see our 2002 report).

kHz software developments: To upgrade SLR Graz with a kHz Laser, a new set of Real-Time tracking, ranging and calibration programs was developed and tested, which allow for completely free running laser pulses, with laser repetition rates from 10 Hz up to kHz ranges.

At 2 kHz, up to about 300 shots are in flight simultaneously to and from high satellites, like *GPS*, *GLONASS* or *ETALON*. The programs have to handle everything within a 500 μs loop: Controlling the telescope, setting range gates, handling start-/stop-pulses, combining the correct pairs, detecting possible returns – at return quotes down to about 0.1% – out of the 2-kHz-Noise, handling the Graphical User Interface, doing all automatic routines (Automatic Return Detection, Automatic Range Gate Setting/Shifting, Automatic Search Routines, Automatic Time Bias settings, Automatic Tracking Optimizations, etc.), and to store all results in real time on disk.

Another problem with kHz laser ranging is the possible coincidence between laser firing and expected return. During the first 50 μs after the laser start, significant backscatter photons are impinging on the detector. If any return photon – and we have to expect mainly Single Photons due to low laser energy – of an earlier laser shot arrives within these 50 μs, the detector might be blocked already by the backscatter noise. With a 2 Hz laser, this situation arises for about 10% of all shots. To avoid this situation, we implemented automatic circuitry into the FPGA chip of the Range Gate Generator, which shifts laser-firing pulses accordingly in case of such a coincidence problem.

First kHz Laser System results: Since October 2003 the kHz Laser System has become operational. Results of the first 10 days show the expected, tremendous increase of data yield: These first 10 days resulted in 120 passes with more than 10 million returns – slightly more returns than in the 6361 passes of the previous 180 days of 2003.

Satellite	Max. Returns 10-Hz-Laser (35 mJ/shot)	Max. Returns kHz-Laser (0.4 mJ/shot)
LAGEOS	14 000	> 200 000
Envisat etc.	5 000	> 350 000
TOPEX	7 000	> 700 000
AJISAI	8 000	> 1 000 000
GPS	About 300/hr	> 10 000/hr

Table 1: Increase of data yield.

Much more important than even these impressive numbers, is the increase of data density in the Normal Points (NP) which are used almost exclusively for SLR data applications. While we achieved about 20-30 data points per NP up to now, with the kHz Laser System we get more than 40 000 points per NP (for most Low Earth Orbit Satellites, see Fig. 2.15). Even for *LAGEOS*, we increased from a previous average of 250 Returns/NP to a maximum of >20 000 Returns/NP. At average, this should result in an improvement of NP accuracy by at least an order of magnitude.

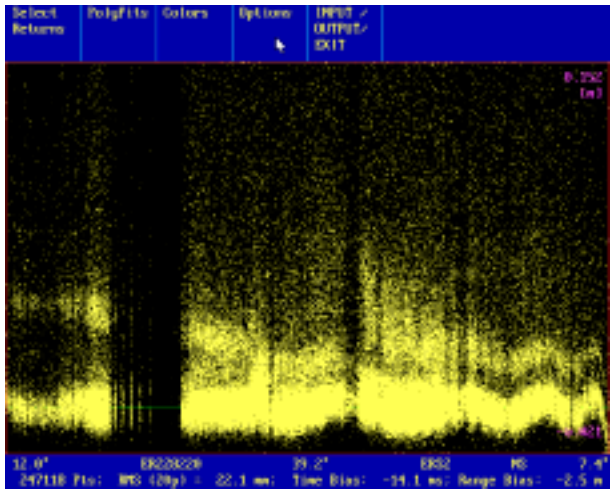

Fig. 2.15: ERS-2 Pass, with about 180 000 Returns; Most returns (at bottom) from the nearest Retro; but from above, returns from another Retro are clearly visible.

The large amount of data within the NP will also allow a much better definition of the NP itself, as it should show the distribution of the Returns within each NP, allowing for example a much more precise definition of mean reflection point, centre-of-mass corrections etc. At present, we have already verified that we can distinguish single retro-reflector responses for various satellites (*GLONASS, TOPEX, ERS-2, Envisat* etc.). These first results are already offering completely new, additional possibilities for SLR, and will certainly trigger new outputs, ideas, research items etc., for Graz as well as for other SLR stations.

3 Near-Earth Space

The physics of the Earth's space environment is dominated by the interaction between the solar wind and the terrestrial magnetic field. The structures that are created in this interaction are: the bow shock, in which the supersonic solar wind is decelerated; a transition layer called the magnetosheath; the magnetopause (the boundary of the magnetosphere) and the magnetosphere itself with its tail where the magnetic field from the Earth's dipole is dominating, and the ionosphere. In principle all these structures are magnetoplasmas, i.e., electrically charged particles (ions and electrons), where electric and magnetic fields dominate the physical processes.

3.1 Missions

In near-Earth space IWF is deeply involved in the *Cluster* mission, launched in 2000 and currently scheduled to run until the end of 2005, which now yields a wealth of new and exciting data. Corresponding data evaluation and analysis has been performed as outlined below in detail. In addition, IWF is presently involved in building instruments for two new magnetospheric missions.

Double Star

Within the *Double Star Project (DSP)*, two satellites are going to study the Earth's magnetosphere on near-equatorial and polar orbits, respectively. The equatorial satellite (TC-1) has been launched successfully on 29 December 2003, the polar one is to follow in summer 2004. *DSP* is a joint effort by China and ESA. More than half of the *DSP* payload has been provided by European PIs. IWF participates in this mission with two experiments, *DSP-ASPOC* to control the electric potential of the equatorial spacecraft, and *DSP-FGM* to measure the magnetic field on both satellites. IWF is also Co-Investigator for the European *PEACE*, *HIA* and *STAFF* experiments and various Chinese experiments. In addition, IWF has set up a European data distribution center for the mission. Further information on the history and objectives of this mission can be found on the IWF website.

After extensive tests with the Engineering Models (EMs) of the instruments in 2002, the following year started with vibration and thermal vacuum testing on the Structural-Thermal Model (STM) of the *Double Star* spacecraft. Most of the hardware efforts in 2003 went into building and testing the Flight Models (FMs) of the instruments. The environmental test program with the first *Double Star* spacecraft TC-1 began in July 2003, by which time all instrument hardware (with some exceptions) had to be delivered to CSSAR in Beijing. The program comprised, as usual, vibration, thermal vacuum, EMC and magnetic tests. Prior to the final delivery, electrical interface tests to the payload data management system (PDMS) were performed at Imperial College, London. The environmental testing of TC-1 was completed in November, and the spacecraft was shipped to the launch site (Xichang) in south-western China. The launch campaign with final integration with the launcher, system testing, fueling, and other launch campaign activities took one month.

Activities for TC-2 followed TC-1 with a shift of about 6 months. By the end of 2003, most

Flight Models of the instruments had been built and tested, and the integration with the spacecraft has started.

The hardware and software activities were accompanied by a series of Interface Meetings with subsections for technical-programmatic issues, the science working team, and the ground data system, which were necessary to co-ordinate the work in Europe and China. The meetings took place in Beijing in March, Paris in July, and Beijing in November 2003.

Flux-Gate Magnetometer (FGM): Unlike most of the other European instruments for *DSP*, *FGM* has been re-designed to accommodate the ITAR (International Traffic in Arms Regulations) requirements and has been built from scratch. After the Engineering Model (EM) has been verified successfully through the pre-integration test in September 2002, the Engineering and Qualification Model (EQM) has been manufactured and went through various qualification tests. In June 2003, the EQM was delivered to China and was integrated to the TC-1 spacecraft for system level tests. In September 2003, the Flight Model (FM) was delivered to China and was integrated successfully into the spacecraft. Fig. 3.1 shows *FGM* integrated on the TC-1 spacecraft.

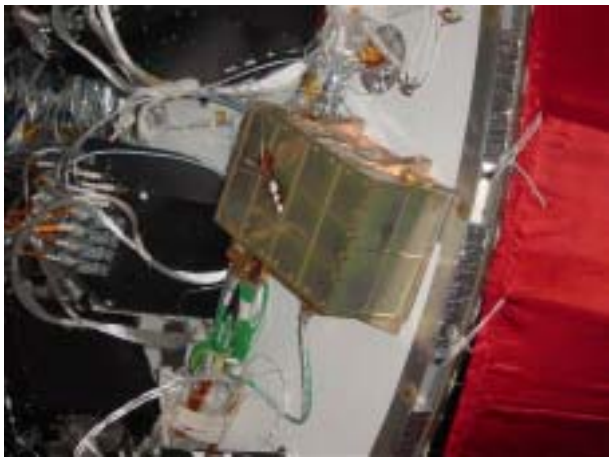

Fig. 3.1: The integrated FGM on board of the TC-1 spacecraft.

In parallel to activities of *FGM* for TC-1, the manufacture and tests of FM-2 (Flight Model for TC-2) is proceeding. The final delivery of FM-2 is scheduled for end of January 2004.

Active Spacecraft Potential Control (ASPOC): The electronics of the FM was completed in April 2003, immediately followed by the integration of the instrument and environmental testing (for vibration at ESTEC and for thermal vacuum and EMC at IWF). A Structural-Thermal Model of the instrument was built and sent to China to participate in the mechanical testing of the STM spacecraft. The *ASPOC* FM was shipped to CSSAR for pre-integration and further system level tests end of June 2003.

In the first half year of 2003, the ion emitters for the FM were produced at Austrian Research Center Seibersdorf, and IWF participated in the thermal and functional characterization of the emitter modules as well as in designing and testing the associated electronics. The final selection of the four emitters for flight was made according to the results of the functional tests after the emitter vibration test at ESTEC in August 2003.

After the environmental tests of the FM with the spacecraft, and before the start of the launch campaign, the *ASPOC* FM was returned to IWF. In a joint activity between ARCS and IWF, the flight emitters were installed and tested. The final delivery of the instrument to CSSAR took place in November 2003.

European Double Star Data Distribution System (EDDS): As part of its commitments for *Double Star*, IWF took responsibility for the implementation of a Data Distribution System as a service for the European investigators. The center is to collect raw science data from the mission and to provide an interface for convenient data retrieval, with some similarities to the *Cluster* data facilities. The DSP Ground Data System with its participants being distributed over Europe and China required intensive testing, all done in 2003.

THEMIS

THEMIS (Time History of Events and Macroscale Interactions during Substorms) is a NASA mission designed to give the ultimate answer to the long-standing question about the causal relationships in one of the most dynamic chain of processes in the Earth's magnetosphere and to the origin of auroral phenomena. In March 2003 it was selected as the next mission in NASA's Medium-class Explorer (MIDEX) program.

THEMIS will be launched in 2006 and fly five identical microsatellites through different regions of the magnetosphere (Fig. 3.2).

Fig. 3.2: Model of the five THEMIS spacecraft in the launch configuration.

IWF will participate in *THEMIS* by providing a magnetometer, which is developed under the leadership of TU Braunschweig. Within the magnetometer team, IWF is responsible for the development of the interface electronics to the instrument processor as well as for the magnetometer calibration, qualification and integration jointly with TU Braunschweig. In 2003, a breadboard model has been assembled and tested and the development of the engineering and testing unit (ETU) has been started.

3.2 Physics

A fleet of spacecraft within the terrestrial magnetosphere and in the near-Earth interplanetary space, like *Cluster*, *Geotail*, *AMPTE*, *Interball*, *Goes*, *Polar*, *ACE*, *Wind*, and others, only to mention the most important of them, provide us with an enormous amount of data representing the plasma and magnetic field behavior in this region. We developed various theoretical models describing physical processes, which are responsible for the formation of structures and phenomena in the near-Earth space. These are e.g., the evolution of the bow shock and the magnetosphere, the reconnection of magnetic field lines at the dayside magnetopause or in the nightside magnetotail and many others. In addition theoretical models are compared with spacecraft data.

Solar Wind

Core-halo distributions are a ubiquitous feature of a variety of different astrophysical systems. In particular, a manifestation of these structures is found in the thermo-statistical properties of the interplanetary plasma. Applying the non-extensive double-kappa distribution to solar wind electron observations generates an accurate representation of the entire velocity space structure with regard to the restricted low-energy core population continuing into the convex and suprathermal halo distribution shape. Based on *WIND* electron observations it turns out that shortcomings of single positive-kappa fits are corrected with an underlying negative-kappa core approach, subject to an enhanced distribution maximum and a reduced distribution width for particle energies just below the core-halo transition. As further significant advantage, best fits are obtained with equal core-halo density and temperature, thus manifesting the relevance of the theoretically derived unique core-halo distribution as ac-

curate representative of the observed velocity space structures with κ being the only core-halo shaping parameter.

Contrary to interplanetary electron distributions, proton velocity space structures typically exhibit a clear separation of the core and halo component peaks in the distribution along the interplanetary magnetic field, where the separation scale was suggested to average around 1.4 times the local Alfvén speed, but in fact is subject to a significant and unexplained spread in velocity space. Upon applying the double-kappa theory to solar wind double-humped proton distribution samples provided by the HELIOS spacecraft, it turns out that the observed structures are particularly well fitted and that the core-halo peak-separation scale follows a maximum entropy condition, instead (Fig. 3.3).

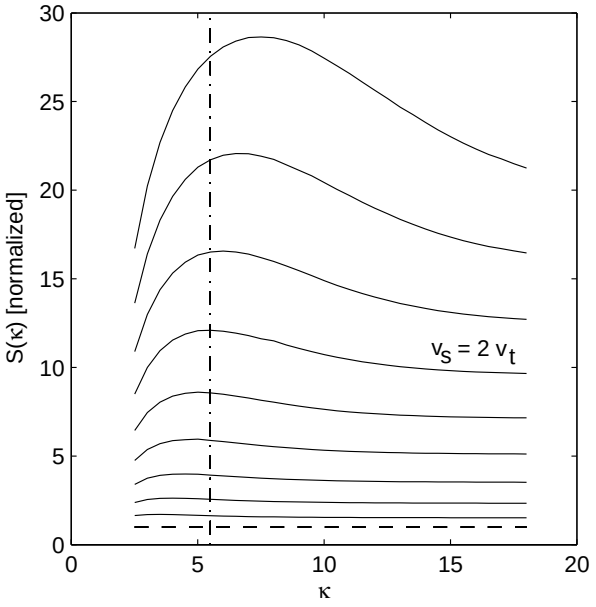

Fig. 3.3: The set of curves corresponds to increasing peak separation scale where the entropy maximum appears for a solar wind $\kappa = 5.5$ at twice the thermal velocity.

Moreover, the thermal cutoff of the core distribution fraction coincides with the halo distribution peak or bulk speed and implies the existence of a critical and relaxed velocity space structure, associated with one uniform particle distribution that is fine-tuned at maximum entropy.

Bow Shock

Based on realistic solar wind kinetic characteristics one finds macroscopic quantities, as parallel and perpendicular pressures, via the second moments of the velocity space distribution, serving along with magnetic field, flow velocity and density as upstream bow shock input parameters in the set of the Rankine-Hugoniot equations. The solution of the system of nonlinear equations returns the modified downstream physical quantities where the decomposition yields the corresponding magnetosheath distributions. This process allows deducing directly kinetic magnetosheath plasma characteristics from undisturbed solar wind conditions. Based on well-established observations of anisotropic solar wind core-halo structures we model the proton component by the family of kappa distributions and allow also double humped conditions, appropriate for intermediate and high-speed solar wind streams. The numerical simulation permits arbitrary upstream solar wind flow and IMF directions with respect to the shock transition layer and provides all characteristics of the velocity space distributions downstream, as anisotropic heating or change of the fraction of suprathermal particle components (Fig. 3.4).

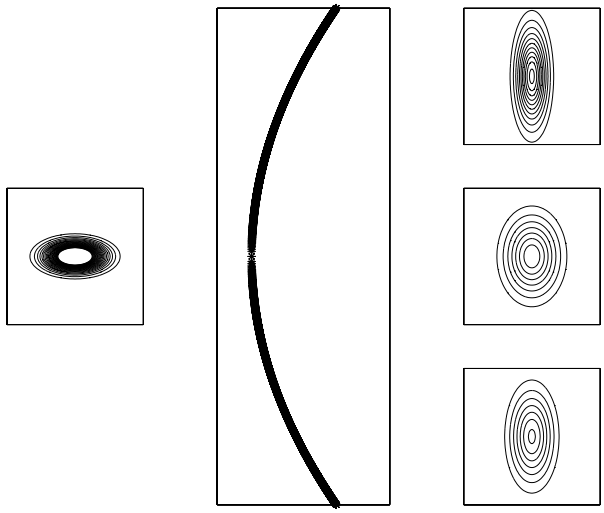

Fig. 3.4: Contour maps of the upstream input distribution and 3 downstream velocity space structures as depending on the shock-normal solar wind flow angle (central panel θ=0°, upper and lower panel θ=5°, θ=20°, respectively).

Magnetosheath

The region of the decreased magnetic field adjacent to the magnetopause is supposed to be produced by a reconnection pulse during which the magnetic barrier energy is converted to a kinetic energy of accelerated plasma flow and heating. With this initial condition we calculate a nonsteady behavior of the magnetic field and plasma profiles between the bow shock and the magnetopause. The build-up process of the magnetic barrier is understood as follows: In the magnetosheath, the solar wind plasma flow produces a stretching of the frozen-in magnetic field lines convecting with the plasma towards the magnetopause. This stretching results in an enhancement of the magnetic field strength in the vicinity of the magnetopause. Finally this process evolves to a steady-state magnetic barrier.

The build-up process for the magnetic barrier is shown in Fig. 3.5, which presents the profiles of magnetic and plasma pressures as well as the kinetic energy density along the subsolar line for different times scaled in units of L_0/u_∞. Here L_0 is the subsolar distance and u_∞ is a solar wind velocity. The pressures and kinetic energy density are normalized to the solar wind dynamic pressure ρu_∞^2. The distances are normalized to L_0. One can see that the plasma pressure minimum and the magnetic pressure maximum are becoming sharper and getting shifted towards the magnetopause. The kinetic energy density is relatively small and its time variation is relatively weak.

The recovery time for the magnetic barrier is obtained as ~2.5 L_0/u_∞, where L_0 is a curvature radius of the magnetosphere at the subsolar point and u_∞ is the solar wind velocity. Considering the magnetic barrier as a background for magnetic reconnection pulses, we estimate for southward interplanetary magnetic field (IMF) a time scale of the reconnection pulse as a ratio of the magnetic barrier thickness ($\approx B_\infty^2/(4\pi\rho_\infty u_\infty^2)$) to the local reconnection speed. The duration of the reconnection pulse is controlled by the IMF, and for a larger B_z component of the IMF, the reconnection pulses can be longer and stronger.

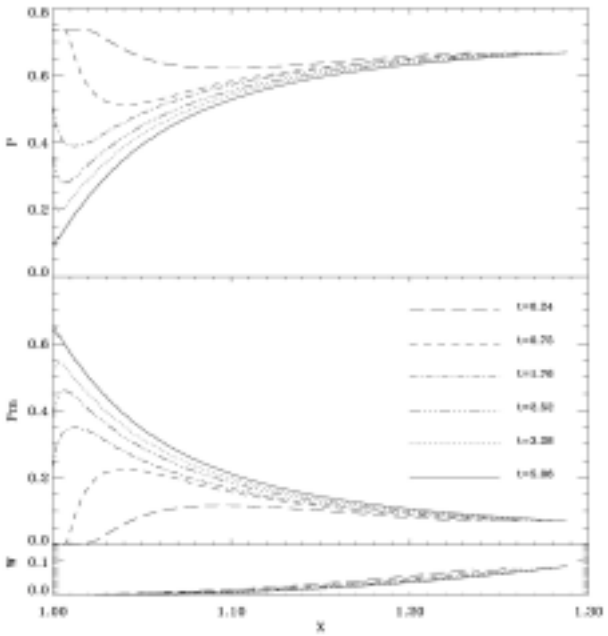

Fig. 3.5: Nonsteady profiles of the plasma and magnetic pressures, and kinetic energy density ($W=\rho u^2/2$) normalized to the solar wind dynamic pressure (ρu_∞^2) along the subsolar line for different times scaled to L_0/u_∞. The coordinate X is normalized to the radius of subsolar magnetopause L_0.

Magnetopause

The inverse problem: Commonly, the border between the terrestrial magnetosphere and the IMF, the so-called magnetopause, is defined at distances from Earth where pressure balance between the solar wind plasma pressure (P_{dyn}) and the magnetospheric magnetic pressure is obtained. However, during times of southward IMF, the phenomenon of magnetic field line reconnection leads to various processes affecting the magnetopause location and shape and starts innermagnetospheric processes. Results of studies on flux transfer events and flux erosion at geostationary orbit will be described in the following.

Flux transfer events are a bipolar variation of the magnetic field component perpendicular to the magnetopause combined with a deflection of the tangential magnetic field components. This phenomenon occurs mainly if the interplanetary magnetic field is orientated purely southwards, and it is a strong indication that magnetic field line merging takes place at the Earth's magnetopause. The characteristic variations of the ambient magnetic field, caused by shocks, which develop due to the reconnection process, were measured by several satellites.

To determine the reconnection rate, which is the characteristic quantity to describe magnetic reconnection, from satellite measurements, it is necessary to solve an ill-posed inverse problem. The mathematical description of the reconnection process is done within the frame of the time-dependent Petschek-type model. The disturbances in the ambient magnetic field, which can be measured by a satellite, are calculated via the so-called Cagniard-deHoop method, which is used in seismology to describe elastic wave propagation. The result of the method gives the magnetic field components as a convolution integral of the reconnection electric field, which is proportional to the reconnection rate, and an integration kernel.

A convolution integral is a well-known problem in the theory of ill-posed inverse problems, and it can be solved by using the theory of regularization. This method enables us to reconstruct different initial reconnection electric field configurations out of magnetic field measurements. It is possible to reestablish the initial electric field out of data, which are measured in a distance of about 50 times the height of the outflow region away from the reconnection site. Additionally, we can model two reconnection pulses, which are separated by a short time period.

Fig. 3.6 shows the initial reconnection electric field and the reconstructed field from a distance of 20 and 50 times the height of the outflow region.

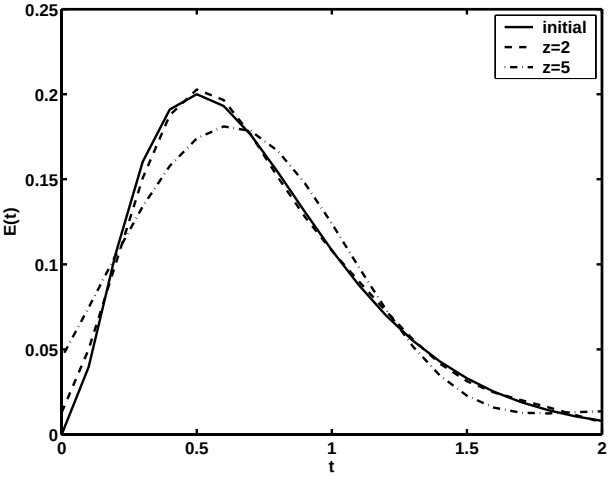

Fig. 3.6: Comparison of the initial reconnection electric field (solid line) and the reconstructed electric field for a distance of z=2 (dashed line) and z=5 (dashed-dotted line).

Statistical survey of erosion at geostationary orbit: As reported above flux transfer events lead to the transport of magnetic flux from the dayside magnetosphere to the nightside during the so-called growth phase of a substorm, commonly known as erosion of the magnetic field. This process can also be observed at geostationary orbit where a depression in the total magnetic field occurs. We studied 288 erosion events around local magnetic noon at geostationary orbit during the years 1996-2001 using solar wind and IMF observations of the spacecraft *WIND* and *ACE* and geostationary magnetic field measurements of *GOES 8, 9,* and *10*. The analysis of the set of data leads to a statistical study of erosion at geostationary orbit as a function of southward IMF. For the investigation of the depression of the geostationary field strength, effects of the solar wind dynamic pressure had to be excluded. Thus, a pressure correction was applied using an analysis of a set of 37 days where no reconnection at the magnetopause took place and no flux was eroded. Fig. 3.7 shows the field depression at geostationary orbit as a function of IMF B_z, where the green line gives a linear fit through all data describing an erosion of the total field (ΔB_z) of 1.67 nT per 1 nT negative IMF B_z.

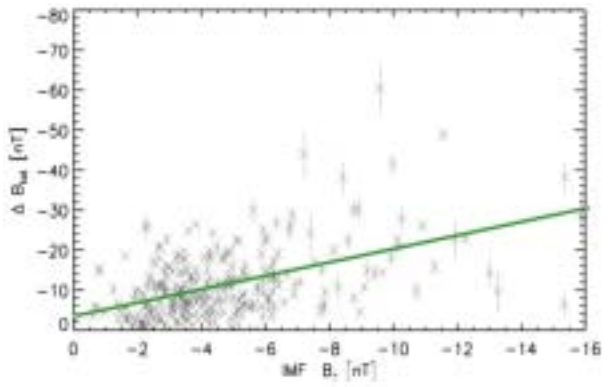

Fig. 3.7: Magnetic field erosion at geostationary orbit as a function of negative IMF B_z. Stars present our set of data with standard deviation for ΔB_{tot}. The green line fits these data from $0 \geq B_z \geq -16$ nT.

Furthermore we performed a bivariate fit, which allows to calculate the total geostationary field strength around local magnetic noon as a function of IMF B_z and solar wind dynamic pressure in a range of $0 \geq B_z \geq -16$ nT and $0 \leq P_{dyn} \leq 6$ nPa. As a result we got a fit, $B_{tot} = 97.64 + 20.22\ P^{1/2}_{dyn} + 1.56\ B_z$.

Magnetotail

At IWF, one of the main research areas is the study of the dynamics of the Earth's magnetotail, with special interest in the transport processes. Data from the four *Cluster* satellites is at the center of the analysis efforts, since they allow to distinguish, for the first time, between spatial and temporal variations of space plasma parameters. This is of particular importance in a highly variable and dynamic region like the Earth's magnetotail and provides a completely new insight into magnetotail dynamics and transport.

The *Cluster* spacecraft were launched in summer 2000 and put into a polar orbit. The orbit of *Cluster* is almost fixed in the inertial frame centered on the Earth. This way they pass the magnetotail from the dawn side flank to the dusk side flank as the Earth's magnetosphere revolves around the Earth once in a year. The tail passes take place from July to October each year. *Cluster* has an almost perfect tetrahedral configuration when it traverses the plasma sheet at its apogee from north to south at a radial distance of about 19 R_E.

Current sheet flapping: Spacecraft traversing the magnetotail plasma sheet frequently observe rapid large-amplitude variations of the magnetic field. These variations, interpreted as up-down oscillation of the current sheet, are known as the current sheet flapping motion. The velocity of this flapping motion exceeds 100 km/s. The flapping may be caused either by the solar wind impact or by internally generated large-scale waves in the current sheet.

The *Cluster* tetrahedron configuration allows determining the normal velocity of the flapping current sheet by multi-point timing analysis. Distributions of Y and Z GSM components of the current sheet normals calculated by a timing analysis for 58 rapid (dt < 300 s) crossings during July-November 2001 are presented in Fig. 3.8a for dawnside and duskside sectors separately.

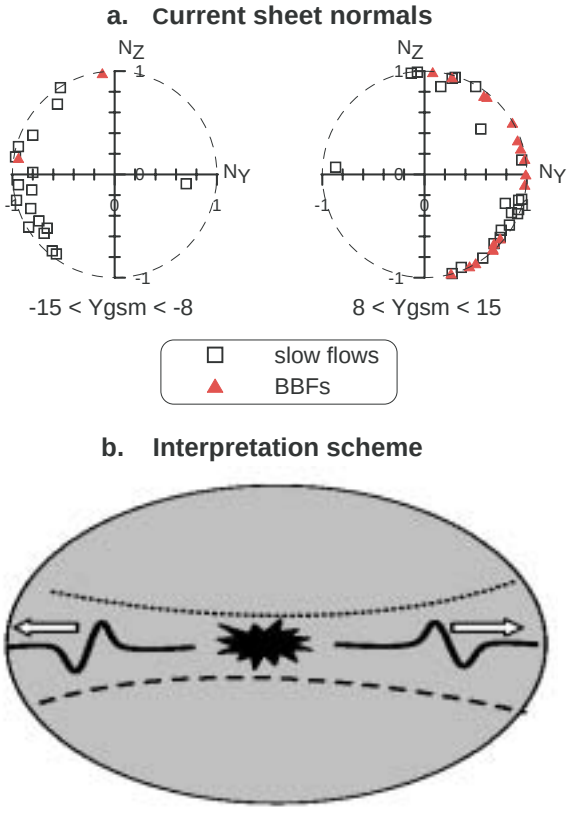

Fig. 3.8: a) Distributions of Y- and Z- components of the current sheet normals for subset of dawnside and duskside crossings during July-November 2001. b) Interpretation scheme summarizing the statistical results.

The results show a strong tendency for the normals to point outward, duskward on the dusk side and toward dawn on the dawn side of the plasma sheet, indicating waves propagating outward from the midnight sector. Hence, the source of rapid flapping waves is localized in the central (near-midnight) sector of the magnetotail. A simple interpretation scheme summarizing the results is presented in Fig. 3.8b.

Kink mode oscillation of the current sheet: On August 22, 2001, *Cluster* observed a giant oscillation of the current sheet (see second panel of Fig. 3.9). This oscillation started approximately 10 minutes before substorm onset (at 0953 UT, based on auroral observations), when the spacecraft started to move out of the magnetotail lobe and into the tail current sheet. It starts with a strong Earthward flow observed by *Cluster* (see top panel of Fig. 3.9. Because of this oscillation the spacecraft cross the center of the current sheet several times. The differences between the crossing times of the four spacecraft can be used to determine the velocity of the current sheet. It moves up and down with a velocity of approximately 10 km/s, and completely reverses its direction (fourth panel of Fig. 3.9). This means that the oscillation is a standing wave and not a traveling one.

The oscillation can be well described by a driven kink-mode oscillation, which was theoretically predicted to exist in a Harris model current sheet. Although it is a standing wave mode, it is not an eigenmode; it is rather driven by the fast flow in the thin current sheet. The result of our modelling can be seen in the third panel of Fig. 3.9. Note how well the model (thick solid line) follows the low-pass filtered data (thick dashed line).

The thickness of the current sheet can be estimated using the x-component of the magnetic field and assuming a Harris current sheet model. We find that the thickness changes very rapidly after the onset of the oscillation (not shown in Fig. 3.9). At the start the thickness is approximately 0.3 Earth radii, but after substorm onset it quickly increases to 2 Earth radii. The thickening of the current sheet occurs on a timescale, which is the same as the damping timescale of the oscillation. This leads us to believe that the oscillation is driven by the fast flow and damped by the thickening of the current sheet.

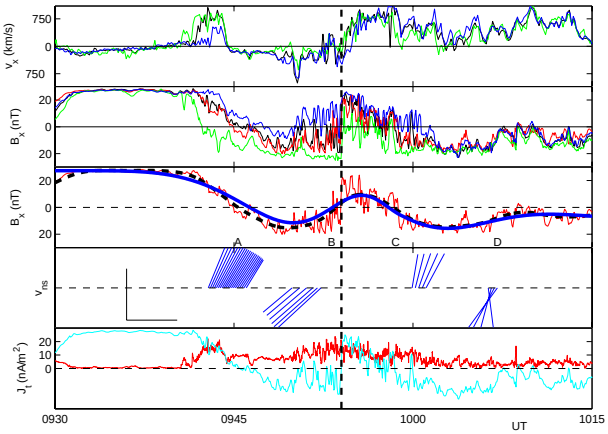

Fig. 3.9: Top two panels show the plasma flow and the magnetic field in the x direction. The middle panel shows magnetic field (thin line), low-pass filtered magnetic field (dashed line) and the modeling of the oscillation (thick solid line). The bottom two panels show the direction in which the neutral sheet moves over Cluster and the x component of the magnetic field (gray) and the total current as measured by Cluster.

Spatial scale of flow bursts: Transient high-speed plasma flow bursts play a major role in mass, energy and magnetic flux transport in the magnetotail. Possible mechanisms for these flows are patchy impulsive reconnection and/or interchange instability of a plasma-depleted flux bubble. With a single spacecraft it is impossible to decide whether the burstiness is caused by spatial or temporal gradients. Using data from plasma and magnetic field measurements obtained by the *Cluster* spacecraft, we could, for the first time, determine the spatial scale of the high-speed flows in the plasma sheet.

For the analysis, we used all bursty flow events during the 2001 tail passes for which at least one of the *Cluster* spacecraft was located in the inner plasma sheet. We concen-

trated on Earthward flows (V_x>0), but since most of those also have a significant dawn-dusk component, we used a new "adapted" coordinate system in our analysis in which the spatial scale of the flow structure is determined perpendicular to the maximum flow direction for each event.

We found that the rate of change in flow speed along the dawn-dusk direction (Y_{mod}, perpendicular to the main flow direction and in the plane of the tail current sheet), is 0.17 per 1000 km, whereas along the north-south direction (Z, perpendicular to the main flow direction and perpendicular to the tail current sheet) it is 0.22 per 1000 km (see Fig. 3.10).

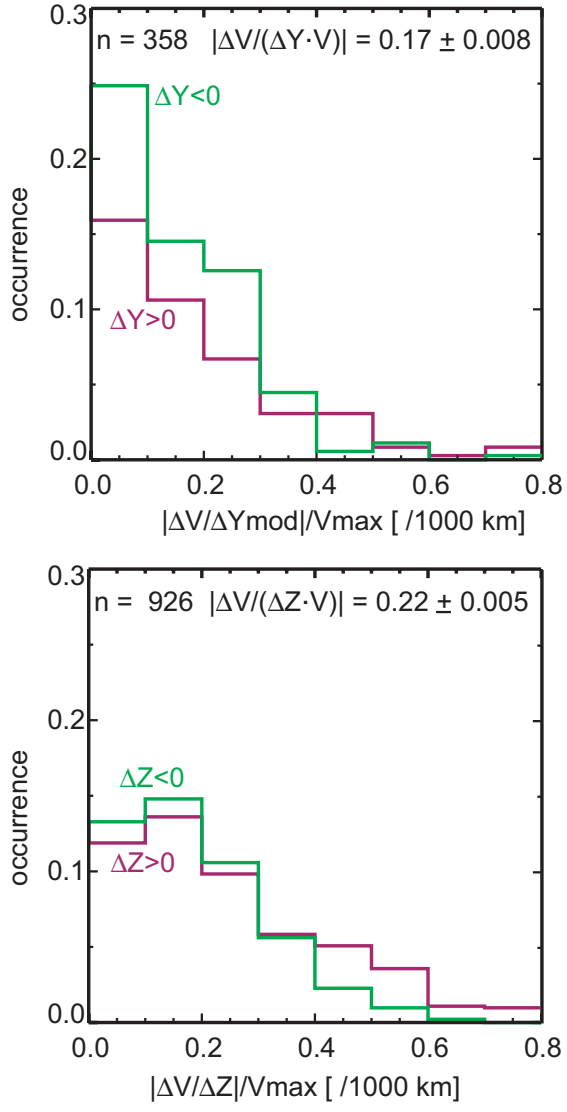

Fig. 3.10: Rate of flow speed change in the "adapted" dawn-dusk direction (Y_{mod}, top) and along the north-south axis (Z, bottom). The rates are normalized to a distance of 1000 km.

These values suggest that the full width of the flow channel is 12000 km in the dawn-dusk direction and about 9000 km in the north-south direction, if we linearly extrapolate this gradient. The scale in Z is similar to typical current sheet widths and suggests that the process causing the bursty flow is related to the tail current sheet, while the scale in Y is comparable to the predicted scale of patchy reconnection from global magnetosphere simulation runs.

Plasma sheet waves: Cluster data is also an excellent source for obtaining very interesting results on the nature of the turbulence in the current sheet. A statistical study of spectral wave power near the neutral sheet has shown that the spectral power is strongly dependent on the plasma flow velocity: the faster the plasma flow, the stronger the turbulence. Up to flow velocities of 400 km/s the increase is steep, but afterwards it flattens, and saturation takes place. However, the spectral index, which describes how the power is distributed in frequency space, remains constant at a value just below 3. This indicates that there is quasi two-dimensional turbulence in the current sheet, driven by a streaming instability, such as the Kelvin-Helmholtz instability, and limited in the third dimension by the finite thickness of the current sheet.

Plasma sheet turbulence: Direct observations of the velocity and magnetic field in the plasma sheet have revealed strong intermittent fluctuations in the temporal and spatial domains. These observations are attributed to turbulence. Contrary to MHD turbulence, e.g. in the solar wind, plasma sheet turbulence is non-steady and the transitory character of driving mechanisms or temporal variations in the boundaries can strongly influence the estimation of turbulence characteristics.

Bursty bulk flow (BBF) associated magnetic fluctuations exhibit multi-scale anisotropy. The time evolution of the relative wavelet power $c_{fr}=c_f(B_Z)/c_f(B_X)$ computed at two differ-

ent scales shows that during BBFs small-scale (0.08 s) magnetic fluctuations appear which are stronger in the vertical direction (Fig. 3.11).

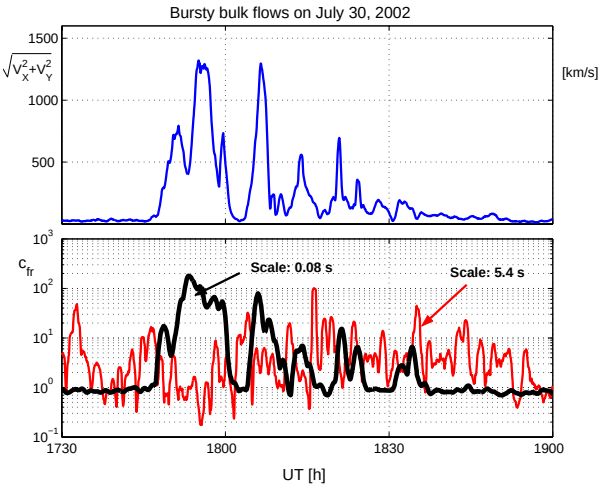

Fig. 3.11: Ion flow speed in the equatorial plane and relative wavelet power at different scales.

Large-scale (5.4 s) anisotropy features are not dependent on the occurrence of BBFs. The observed scale dependent anisotropy can be explained by velocity shear. Furthermore, small-scale magnetic turbulence is non-homogeneous, exhibiting multifractal statistics.

Further studies using *Cluster* data are done on the topics of current sheet structure and lobe convection (both extension of work reported on in earlier Annual Reports), and on substorm dynamics (together with *Geotail* data).

Terrestrial Radio Emissions

The investigation of the quasi-periodic (so-called QP) structures observed in the Earth's plasmasphere by the *Cluster WBD* experiment (Fig. 3.12) focused on three events with the aim to analyze and to determine their spectral features: July 9, 2001, October 21, 2001, and March 25, 2002. Different from previous findings we have seen that the QP structures comprise a frequency range up to 8 kHz and, not yet observed until recently, that these structures simultaneously occur with hiss. This fact opens new possibilities regarding the explanation of the QP generation mechanism.

Particular emphasis was devoted to examine and to outline the instrumental polarization aspects used to investigate radio wave modes. It is well known that the polarization measurements are powerful techniques for studying the magnetized space plasma, in particular for the development of theoretical models for the generation and the propagation of radio waves. Because of this, it is interesting to analyze and compare previous experiments, which were used to derive wave modes in particular in the auroral regions of the Earth's magnetosphere. Within the frame of this analysis (a) the reception systems (i.e. antenna and receivers), (b) the basic methods describing the polarization parameters of the radio waves, and (c) the application of these methods to the observations of Auroral Kilometric Radiations (AKR) have been studied. Corresponding comparisons between *Cluster WBD* and *Interball POLRAD* have been performed.

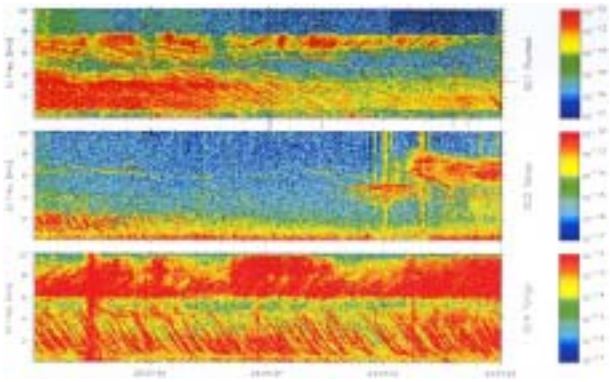

Fig. 3.12: Very Low Frequency (VLF) emissions observed on October 21, 2001 by the Cluster WBD experiment.

4 Solar System

In continuation of previous studies IWF is engaged in many missions, experiments and corresponding data analysis of a multitude of solar system phenomena. The physics of the Sun as central star with an expanding atmosphere, the so-called solar wind, its interaction with solar system bodies (magnetized/ unmagnetized, planets, comets), and various kinds of planetary atmosphere/surface/subsurface interaction phenomena are under detailed investigation.

4.1 Sun

Specific parts of the complex dynamics within the low solar corona have been modeled and simulated by a magnetohydrodynamic approach, as outlined below. Additionally, the Sun was also observed and investigated as emitter of radio waves, generated over a wide radial range along coronal structures, which are heavily influenced by energetic particle beams and shock structures.

Physics

Solar decametric radio emission: Recent measurements of solar Type II radio bursts during the C4 campaign (2002) at the world largest radio telescope UTR-2 (Ukraine) yielded new insights in the fine structure of these bursts associated with shock processes in the solar corona. One typical event of a Type II burst with herringbone structure was registered on July 7, 2002 (Fig. 4.1). The interesting feature is the difference in drift rates of negative and positive sign. The back-bone radio emission exhibits a wave-like structure. This fact can be interpreted as a shock intersecting coronal structures, which are elongated in radial direction out of the Sun. For the first time this provides the opportunity to estimate the involved plasma parameters of these structures from radio observations.

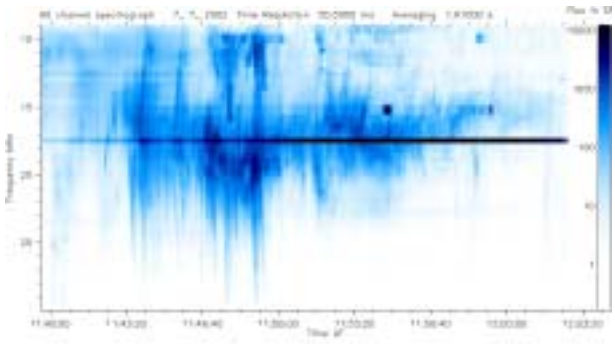

Fig. 4.1: Type II burst with herringbone structure and waving backbone. Fundamental radio emission of this Type II burst is visible close to 10 MHz.

Spectral analysis is performed on a series of measurement campaigns at Graz Observatory Lustbühel radio station, to derive the observed parameters such as the relative intensity, the time duration, the frequency bandwidth, and the drift rate of solar Type III bursts. The results of these studies provide an overview of the observed parameters (e.g. statistical methods) and on the development and the expansion of the Type III burst inside the solar corona. Focussing on the Type III time duration, it is shown that the corresponding histogram could be fitted using two Gaussian distributions. Each one is due to a specific effect, which occurs during the excitation and the damping phases of Type III bursts. Two main parts could be considered: (a) an excitation phase of about 3.9 ±1.5 sec of the Type III burst at its origin in the solar corona plasma, and (b) a damping effect which exhibits a longer time interval (i.e. 9.6 ±2.5 sec). Such studies give more information

about the generation and the propagation of accelerated electron particles along open magnetic field lines emanating from the Sun.

Another observation campaign (C3) was devoted to the Sun observations during the maximum of the 23rd solar cycle in the year 2001. Fig. 4.2 shows a particular solar decametric emission recorded on May 19, 2001 where bursts and fine structures with different drift rates were observed by the digital spectropolarimeter (DSP) at the UTR-2 radiotelescope (Ukraine).

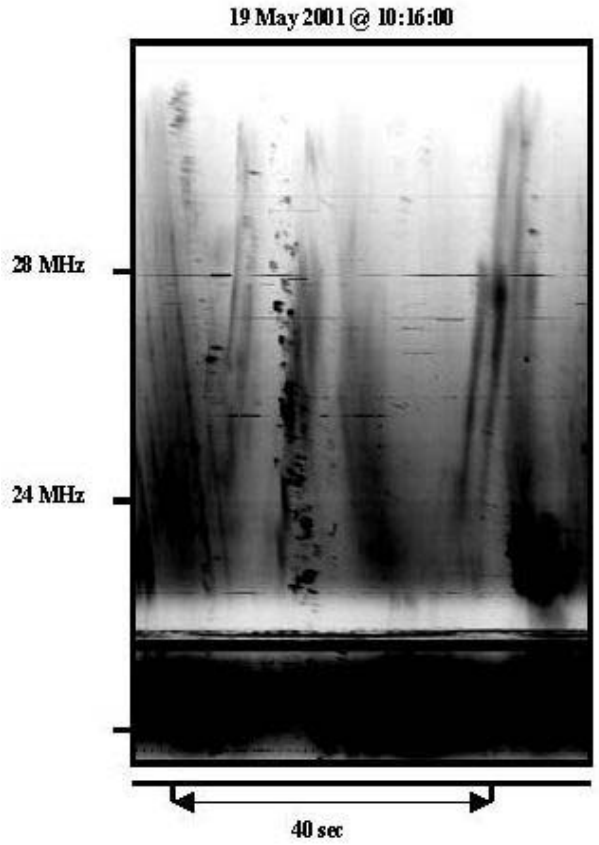

Fig. 4.2: Example of solar decametric emissions recorded during the maximum of the 23rd solar cycle. The solar bursts and fines structures were observed on May 19, 2001 at the Kharkov radiotelescope.

Observations recorded at the UTR-2 radiotelescope (Ukraine) have revealed a number of interesting fine structures within the frequency range from 8 to 32 MHz. We can distinguish two groups: the classic solar drift bursts (e.g. drift-pairs, split pairs, Type I, II, III), and a variety of unusual microstructures, which are under investigation.

Coronal mass ejections: Coronal loops, which trace closed magnetic field lines, appear as the primary structural elements of the solar atmosphere. Complex dynamics of the loops together with under-photospheric dynamo mechanisms cause the majority of coronal magnetic loops to be very likely current-carrying structures. In that connection none of the loops can be considered as isolated from the surroundings. The concept of models under investigation employs the ideas of possible *inductive* and *ponderomotoric* interaction between the electric currents confined within the magnetic loops moving relative to each other. The main attention was paid to (a) oscillations of the loops in active regions and (b) acceleration of solar Coronal Mass Ejections (CMEs), including the associated generation of energetic particles.

Recent high-resolution observations of the imaging telescope on board the *Transition Region and Coronal Explorer (TRACE)* spacecraft provided a view of the variety of decaying transversal oscillations of coronal loops. An oscillatory behavior of the loops is traditionally interpreted in terms of standing or propagating MHD waves. This approach has however difficulties in the explanation of the observed relatively fast decay of oscillations. Our model, based on the effects of ponderomotoric interaction of inductively connected coronal currents, allows to resolve the existing difficulties of MHD-wave models and well reproduces the main characteristics of the oscillatory dynamics of coronal loops.

CMEs are powerful eruptions accompanied by an ejection of significant amounts of the solar coronal material into the interplanetary space. We model a CME as a large rising current-carrying magnetic loop, which interacts inductively with the neighboring loops. Acceleration of CME in our model takes place due to ponderomotoric interaction of electric currents in the CME filament and the system of underlying loops (Fig. 4.3).

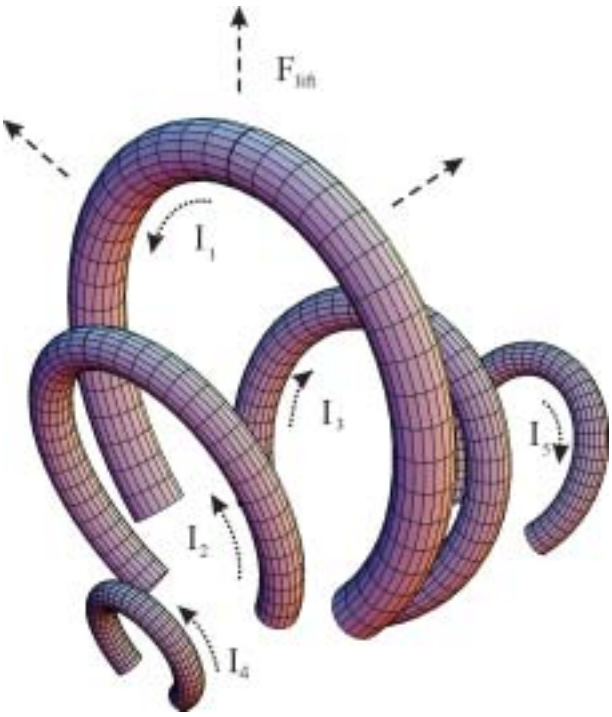

Fig. 4.3: CME as a rising and expanding magnetic loop above the group of loops.

The dynamical solar corona in 3D consists of transient type magnetic island elements and radial type magnetic flux rope structures. During formation and relaxation these elements produce inductive electromagnetic fields, which generate energetic particles. Beams of energetic particles excite at high frequencies Type I and Type III radio storms.

Based on the methods of plasma kinetic theory developed for the hot current-carrying plasmas a theoretical approach to model a 3D solar corona formation has been proposed. A 3D dynamical structure of the corona with diamagnetic and resistive currents is formed as a result of relaxation or instability of the 2D initial diamagnetic state.

Electric fields, which accelerate plasma particles, are studied with two mutually perpendicular wave vector orientations forming cases of tearing and stratification modes. The tearing mode characterizes the formation of radially moving transient or CME type magnetic islands, while the stratification mode forms radial magnetic ropes or rays.

4.2 Mercury

Mercury is the planet nearest to the Sun. It is a significantly dense planet, which suggests a large iron core and possesses a weak global magnetic field. The planned ESA mission *BepiColombo* to Mercury will explore the planet in detail and over a longer period of time in the coming.

BepiColombo

BepiColombo is a space mission to Mercury. It is new and special in several ways. Not only is it the first joint European-Japanese space project, in which both ESA and the Japan Aerospace Exploration Agency (JAXA) are participating, it is also the first time that two orbiters are flying to this innermost planet.

Within the scope of the European-Japanese *MERMAG Consortium*, IWF will participate in proposals for magnetometers on both spacecraft. IWF will be in charge of the *MERMAG-M* magnetometer on the Japanese-built *Magnetospheric Orbiter*. IWF will also participate in a consortium for a particle analyzer on board of ESA's *Planetary Orbiter*.

4.3 Venus

Venus, like other planets in the solar system, is under the influence of a continuous flow of charged particles from the Sun, the solar wind. However, the lack of an intrinsic magnetic field makes Venus a unique object to study the interaction between solar wind and the planetary body. The planetary body has a dense atmosphere, but no magnetic field, thus the solar wind interacts directly with the upper atmosphere. The absence of a planetary magnetic field leads to important differences between Venus' and Earth's atmospheric escape and energy deposition processes. The upper atmosphere of Venus is not protected by a magnetic field from direct interaction

with the solar wind. Fig. 4.4 illustrates associated electrodynamics processes and plasma domains of the Venus upper ionosphere.

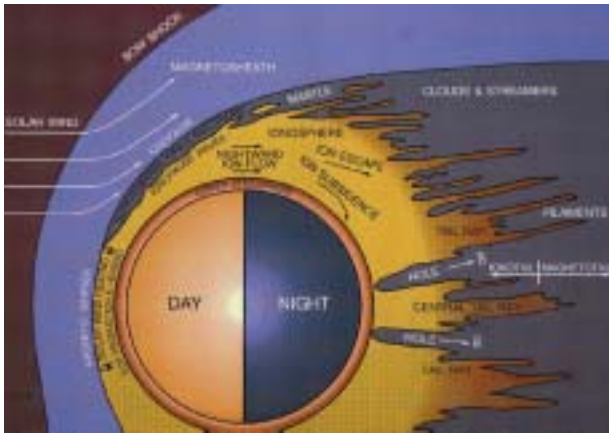

Fig. 4.4: Solar wind-ionosphere interaction at Venus.

The earlier missions, *Venera* and *Pioneer* orbiters, found that the current induced by the solar wind electric field forms a magnetic barrier that deflects most of the solar wind flow around the planet and leads to the formation of the bow shock. The ionosphere is terminated on the dayside, developing rapid antisunward convection and tail rays. However, the short lifetime of the *Venera* orbiters, and insufficient temporal resolution of the *Pioneer* plasma instrument did not allow a study of the mass exchange between the solar wind and the upper atmosphere of Venus and energy deposition to the upper atmosphere in sufficient detail.

Venus Express

Venus Express is an ESA mission to Venus with the re-use of the *Mars Express* spacecraft platform. IWF takes the lead on one of the seven payload instruments, the magnetometer.

The magnetometer aboard *Venus Express* will map the magnetic properties in the magnetosheath, magnetic barrier, the ionosphere, and the magnetotail. It will be instrumented to identify the plasma boundaries between the various plasma regions and to study the solar wind interaction with the Venus atmosphere.

In 2003, the manufacturing of the Engineering Model (EM) was completed. It was delivered to Astrium, Toulouse, where it was integrated into the spacecraft simulator for further tests (Fig. 4.5). All the EM tests have been successful so far. Following the delivery of EM, the production of the Qualification Model (QM) has been completed and is undergoing various functional and environmental tests.

In parallel to the hardware activities, attention has been taken on the data processing of the magnetic field measurement. A strayfield test has been performed on the *Mars Express* spacecraft and the data has been carefully analyzed in order to improve the calibration software capability.

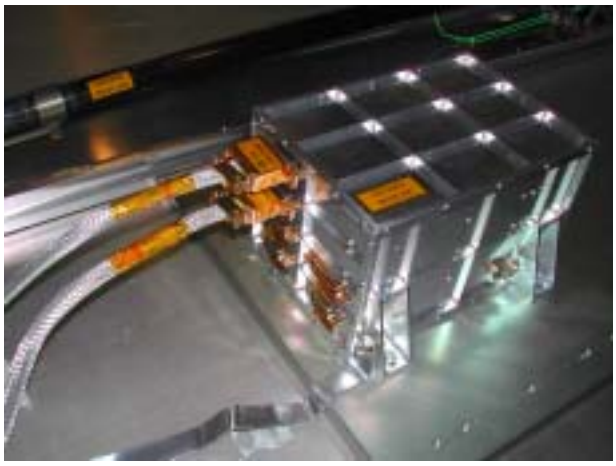

Fig. 4.5: The MAG EM being integrated into the test bench at Astrium, Toulouse.

Physics

Atmospheric loss processes like Jeans escape, the production of energetic “hot” neutrals by dissociative recombination of ionospheric constituents, atmospheric sputtering, ion pick up and the production of detached plasma clouds caused by plasma instabilities were studied at the Venusian atmosphere-ionopause regime. It was found that charge exchange and dissociative recombination produce hot H and O populations in the upper atmosphere. By using a Monte-Carlo technique for the simulation of hot atom diffusion processes through the Venusian atmosphere

an escape rate of about 2×10^{25} s^{-1} for hot H atoms was calculated. This escape flux may even be higher, because the escape of hot H atoms could be much higher due to the uncertainty of the photochemical relevant H_2 number density in the Venus nightside. Our study suggests that the escape flux for hot O atoms is negligible at Venus but the particles reach high altitudes via ballistic trajectories as shown in Fig. 4.6, where they can get ionized and picked up by the solar wind plasma flow.

By estimating the atmospheric sputter yield for oxygen atoms and a flux of coronal O^+ pick up ions, which can again enter the Venusian atmosphere of about 1.3×10^6 cm^{-2} s^{-1} we found a very small escape rate for sputtered O atoms in the order of about 10^{22} s^{-1}. The total loss of planetary pick up ions was estimated by means of a test particle model, which is based on the proton flow in the magnetosheath according to the Spreiter-Stahara model. Once the production rates of planetary ions due to photo ionization, electron impact and charge exchange are determined by using the neutral density profiles shown in Fig. 4.6, escape fluxes for planetary ions in the order of about 1.5×10^{25} s^{-1} (H^+) and 5×10^{24} s^{-1} (O^+) were calculated. The ion loss rate for O^+ is comparable with measurements of the *Pioneer Venus Orbiter*, indicating large plasma clouds, which became detached from the ionosphere due to some kind of MHD instabilities. Our preliminary results suggest that contrary to Mars, only solar wind induced ion loss processes are relevant for the loss of heavy atmospheric constituents. The ratio between H:O escape to space is much closer to the ratio of 2:1 than at Mars.

Our results are of relevance in view of the upcoming *VEX-MAG* and *ASPERA-4* observations aboard *Venus Express*. A corresponding study, performed together with the Swedish Institute of Space Physics in Kiruna, compares the energetic neutral atom (ENA) production from the ion distribution and fluxes around Venus between the Spreiter-Stahara and the Biernat-Erkaev plasma flow model.

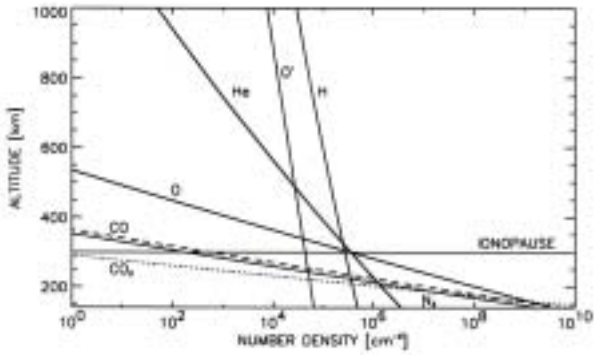

Fig. 4.6: Calculated density profiles for thermal and hot atmospheric gases.

4.4 Mars

The planet Mars continued to be in the focus of research activities in 2003. New investigations concerning a possible participation in ESA's planned *ExoMars* mission have been started. Model calculations concerning the behavior of ice melting probes that might be developed in the foreseeable future to explore the vertical structure of the Mars polar caps have been performed. The theoretical studies concerning the UV and particle fluxes and their influence on atmospheric loss mechanisms have been continued and extended. Regarding the search for water extensive studies have been performed on the reception properties of the *MARSIS* radar antenna system (see 5.2).

Physics

Surface-atmosphere interaction: An estimation of the present and past surface water-ice reservoirs, which have been in exchange with the Martian atmosphere, was carried out by using observed Deuterium (D) and atomic Hydrogen (H) ratios in atmospheric water vapor, Martian meteorites and isotope ratios based on asteroid/cometary impact delivery to early Mars. By using initial D/H ratios of about 1.2 to 1.6 times the Terrestrial Sea Water (TSW) ratio, one gets a present water-ice

reservoir equivalent to a global ocean layer about 3.3 to 15 m thick. By assuming that hydrodynamic escape fractionated the D/H ratio before 3.5 Gyr (3.5×10^9 years) to a value as found in SNC meteorites, we estimate a present water-ice reservoir layer with a thickness of about 11 to 27 m. From the obtained range, a water-ice reservoir layer of about 17 to 60 m should have existed 3.5 Gyr ago. The estimated reservoirs depend on the escape of water since 3.5 Gyr ago equivalent to a global ocean with a thickness of 15 to 35 m.

The main uncertainties between minimum and maximum are related to present uncertainties of the efficiency of atmospheric loss rates triggered by plasma instabilities and momentum transfer effects between the solar wind and the ionosphere. We investigated the growth rate for the Kelvin Helmholtz (KH) instability at the Martian ionopause and found that this instability may evolve into a nonlinear stage at the whole terminator plane, but preferably at the equatorial flanks (Fig. 4.7). Escape rates of O^+ ions ($\approx 1024\ s^{-1}$) due to detached plasma clouds implicate that loss by instabilities should be comparable with other loss processes studied by the *ASPERA-3* instrument on board of *Mars Express*.

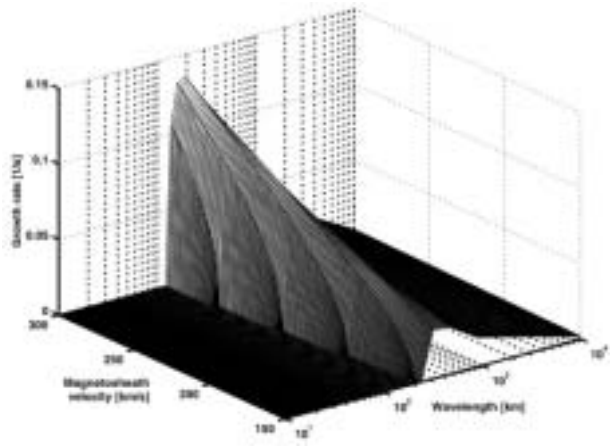

Fig. 4.7: Instability growth rate for a Martian ionopause altitude of 400 km and a solar wind velocity of 400 km/s at the flanks near the terminator plane.

Further a study was carried out, which analyzed the efficiency to sequester atmospheric oxygen in the course of oxidative weathering of the global Martian dust. The role of chondritic meteorite dust was investigated by means of a least squares analysis of chemical data obtained from *Pathfinder APXS (Alpha-Proton X-Ray Spectrometer)* and *Viking XRFS (X-Ray Fluorescence Spectrometer)* measurements.

A three-dimensional regression analysis of oxidation states suggests that the meteoritic fraction is the main sink for atmospheric oxygen. The result of this study is consistent with recent laboratory experiments carried out by NASA and may imply that Mars' rusty red color could also be produced by chemical reactions between atmospheric oxygen and infalling meteoritic dust without a humid water-rich atmosphere.

Electromagnetic sounding of the Martian atmosphere by Schumann resonances: Natural electromagnetic waves produced near the Martian surface by electrostatic discharge in dust storms (dust devils) or geological activity can be trapped in the resonant cavity formed by the surface and upper ionosphere, as it occurs on Earth. Low frequency electromagnetic waves can also travel along the magnetic field lines of the recently discovered magnetic anomalies from the magnetosphere to the surface and may produce resonant structures in the cavity. The measurements of resonant frequencies, also called Schumann frequencies, by surface stations can be used for remote sensing of the electrical conductivity of the lower ionosphere/atmosphere. The structure of the Schumann resonances is mainly determined by the geometry of the cavity and the global electrical conductivity of the ionosphere/atmosphere. We used a numerical model of electromagnetic wave propagation based on the Transmission Line Modelling (TLM) method with the aim of calculating the resonance frequencies on Mars. Due to the high atmospheric conductivity close to the ground, the resonances are very smooth and have a fundamental mode with a frequency of

11 Hz. The first two resonances at 11 and 22 Hz are very clear (Fig. 4.8). Their magnitude and relative intensity depend on solar conditions and could be also a tool to detect the existence of meteoroid layers in the ionosphere. The model has been previously validated by application to the terrestrial case.

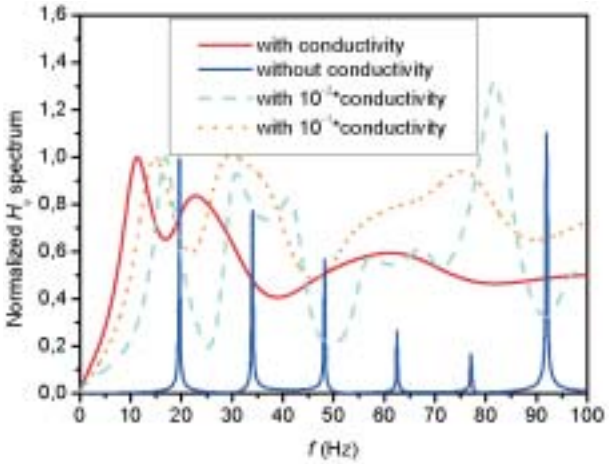

Fig. 4.8: Simulated Martian Schumann spectra for various conductivity profiles.

4.5 Jupiter

One of the most intriguing solar system phenomena is the Jupiter-Io interaction leading to triggered non-thermal radio emission. Specific emphasis was put on the microstructure of the Io-triggered S-bursts.

Jupiter Radio Observations

Jovian decameter millisecond or S-burst radiation represents a unique phenomenon in the planetary emission. S-bursts manifest themselves as a series of short pulses with durations from a few to tens of milliseconds and are strongly controlled by the Jovian satellite Io. They have a number of important properties, such as their spectral form, rapid drifts in the frequency-time plane, "fine" temporal and frequency structure, narrow-band events and apparently an internal structure in form of subbursts which for the first time have been verified by waveform receiver recordings and subsequent wavelet analysis.

The recent development of the so-called waveform receiver (WFR) at IWF is a successful step forward enabling the detection of S-burst substructures. By capturing the waveform rather than the derived dynamic spectrum, post processing tools allow the application of various methods for this signal substructure analysis. Especially the method of wavelet transformation turned out to be very effective, when dealing with intrinsic signal information.

In Fig. 4.9 an example of the simple S-burst emission wavelet spectrum is shown (a segment of about 5 ms with an initial data sampling rate of 50 MHz). This signal was recorded during an Io-C storm on February 26, 2000, by the waveform receiver installed at the UTR-2 telescope Kharkov (Ukraine).

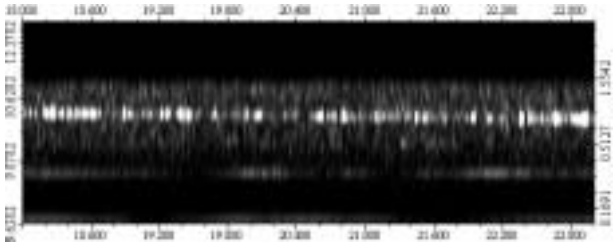

Fig. 4.9: The wavelet spectrum of the simple S-burst (time interval is from 18-23 ms, initial sample rate 50 MHz, time length of used complex Morlet mother-wavelet is 3 μs) with high time resolution.

For the first time this observation provided a view into the internal structure of an S-burst signal consisting of very narrow ("superfine") pulses with individual time duration 6-15 μs, which in turn, are grouped from 20 to 150 μs. The instantaneous frequency band of one separated microsecond pulse was determined to comprise 100-300 kHz. Thus, an instantaneous frequency band of emission is in the order of 200 kHz, and the excitation increment of instability, which is supposed to be the cause of the decameter S-burst generation, has a narrow frequency band $\Delta f/f \approx 10^{-2}$.

It was also found that one separate pulse occupies a certain frequency interval, but has practically no clear expressed frequency drift in time. It seems that the frequency drift of

the simple straight burst as a whole results from sequentially decreasing frequencies over the time for each subsequent pulse. These findings have important implications on the development of an improved S-burst generation mechanism theory.

Simultaneous spacecraft radio observations: Jovian DAM (decametric) and HOM (hectometric) radio data recorded by the *Galileo* spacecraft (*PWS-HFR* receiver) in orbit around Jupiter and the *WIND* satellite (*WAVES-RAD2* receiver) in Earth's orbit from the period 1996-2000 were used to derive parameters of the specific emission geometry during times of simultaneous observations.

Fig. 4.10 shows an example of a simultaneously recorded intense Jovian decametric spectral arc structure (indicated by red arrows), which can be tracked from 13.825 MHz in the *WIND* spectrum (upper image) down to a few hundred kHz in the *Galileo* spectrum (lower image).

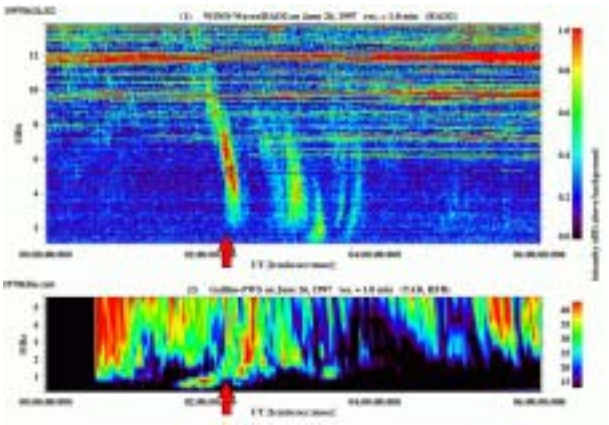

Fig. 4.10: An example of a Jovian DAM spectral arc recorded simultaneously by WIND (upper spectrum) and Galileo (lower spectrum) between 01:40 UT and 02:20 UT, on June 26, 1997.

From these simultaneous recordings an interesting result has been achieved with respect to the apparent semi-apical angle of the radiating hollow cone structure. This angle exhibits an almost identical value of ~46° for the two best simultaneous recordings of a DAM spectral arc between *Galileo* and *WIND*.

4.6 Titan

Titan, the Earth-like moon of Saturn, will be investigated by the joint NASA/ESA mission *Cassini/Huygens*. The planetary probe *Huygens* will descend to Titan's surface in January 2005 and the *Cassini Orbiter* will investigate the Saturnian System for several years.

Cassini/Huygens

The joint NASA/ESA mission *Cassini/Huygens* will start after a seven years journey to investigate the Saturnian system in mid 2004, when the spacecraft is injected into an orbit around Saturn. In January 2005 the planetary probe *Huygens* will descend to Titan's surface. IWF participated in the design and development of the following instruments onboard the spacecraft: *Huygens Atmospheric Structure Instrument (HASI)*, *Aerosol Collector and Pyrolyser (ACP)*, and the *Cassini Radio and Plasma Wave Science Experiment (RPWS)* aboard the *Cassini* orbiter.

Physics

Schumann resonances at Titan: The *Huygens Atmospheric Structure Instrument (HASI)* will measure low frequency electric fields in Titan's atmosphere. Theoretical investigations of the so-called Schumann resonances, which are global resonance patterns of the waveguide bounded by the surface and the ionosphere, were performed. The dependence of the frequencies on ionospheric conditions was analyzed based on a study for Earth conditions, were a wealth of data exist. They were compared with theoretical and experimental results of the commonly used two-scale height ionospheric model and for a model with high-energy particle precipitation at the terrestrial poles. The simulations agree very well with experimental findings and the first Schumann resonance frequency slightly increases associated with the dimensional re-

duction of the waveguide during particle precipitating events. Similar high-energy particle effects are expected for the interaction of the Saturnian magnetospheric wind with Titan.

Additional theoretical investigations concerning the waveguide have been worked out in the framework of the classical two-scale height ionospheric model and for arbitrary profiles. In particular, the Schumann resonance spectra for a point source depend on the source-observer distance (polar angle). The results show that for favorable ionospheric conditions the resonance peaks are clearly visible, whereas for higher conductivities, equivalent to larger wave damping, the higher frequency peaks almost disappear in the background noise.

In order to calibrate the *Huygens HASI* and radar experiments, the Italian Space Agency (ASI) organized a balloon test flight in June 2003 in Sicily, where IWF participated with electrical measurements. A spare model of the *HASI* experiment was used and the data obtained during the five hours flight were investigated to determine the influence of the balloon and the *Huygens* mock-up on the measurements of the electrical conductivity and the low frequency electric fluctuations, including Schumann resonances.

The reconstruction of the Huygens entry and descent trajectory: The *Huygens* probe will be released from *Cassini* on December 24, 2004 and enter the atmosphere of Titan on January 14, 2005. During both the entry and descent phase the probe will perform scientific measurements to determine the physical properties of Titan's atmosphere, measure winds and global temperatures, and investigate energy sources important for the planet's chemistry.

To correctly interpret and correlate the results from all the probe science experiments and to provide calibration opportunities for synergistic studies with orbiter remote sensing instruments, an accurate reconstruction of the probe entry and descent trajectory is needed.

The *Huygens* Descent Trajectory Working Group (DTWG) is co-chaired by IWF since January 2003. IWF has the responsibility to develop, implement, and validate the necessary algorithms by the time of the probe mission.

The *Huygens* mission can be subdivided into the entry and the descent phase. The entry phase commences at the interface altitude of 1270 km above the surface of Titan and ends at the start of the parachute sequence (Fig. 4.11). During this phase the probe will only measure the aerodynamic deceleration, which can be used for the numerical integration of the equations of motion to yield the probe position and velocity and infer the atmospheric properties like density, pressure and temperature.

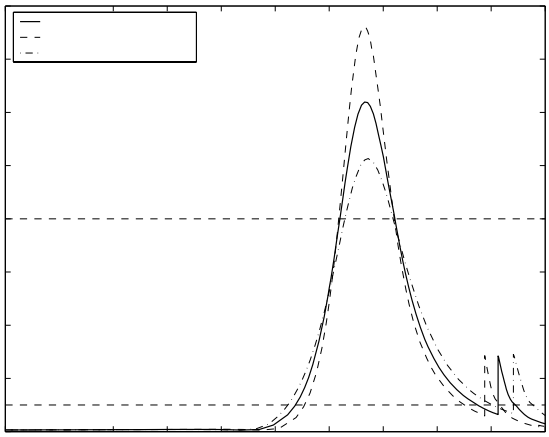

Fig. 4.11: Simulated Huygens probe deceleration for the nominal and maximum Yelle Titan atmosphere model; T_A = triggering of the parachute sequence arming timer, S_0 = probe onboard software (POSW) descent timer start, and T_0 = parachute sequence deployment.

During the descent phase, the pressure and temperature measurements by *HASI* will be used for the trajectory reconstruction. The deployment of the parachute sequence at ~160 km altitude will most likely introduce some oscillatory motions into the spacecraft-parachute system and hence into the measured accelerations as well.

The numerical integration of the probe acceleration measurements, the reconstruction of

the physical properties of the upper atmosphere as well as the *HASI* pressure and temperature measurement conversion have been successfully implemented and tested using simulated *Huygens* instrument measurements and data sets from past probe missions (e.g., *Mars Pathfinder*). The development of a sequential estimation algorithm (i.e., a Kalman filter) has started and will enable an update of the reference trajectory in order to provide a "best combination" of all available data sets.

4.7 Comets

Comets are considered to have their origin in cool and distant regions of our solar system at very early stages of its evolution. Thus, cometary matter might have preserved some original signatures of the materials at that time. The scientific interest in comets is characterized by their dual role as messengers from the beginnings of the solar system and as relatively unexplored, "exotic" small bodies. So far, our current knowledge is based on the cometary missions to comet Halley in the late 1980's, which were not more than a quick snapshot of a cometary nucleus.

Rosetta

ESA took a lead in closing some of the knowledge gaps by assigning a cornerstone mission to the exploration of a comet in all detail by measurements in-situ. This mission, labeled *Rosetta*, will monitor the evolution of a comet during its approach nearer to the Sun over a long period of time from an *Orbiter*. In addition, a *Lander* will be dropped on the surface of the nucleus.

Due to problems with the Ariane-5 rocket, the launch, which was foreseen for January 2003, was postponed to February 2004. Furthermore, *Rosetta* can no longer reach its original target, comet P/Wirtanen, and will fly to comet 67P/Churyumov-Gerasimenko instead.

IWF participates in a number of experiments in this key ESA mission. It is leading the investigation of dust particles collected in the coma by means of an atomic force microscope. This instrument *MIDAS* on the *Rosetta Orbiter* is to investigate the structure, flux and magnetic properties of the grains. IWF also contributes to the mass spectrometer *COSIMA* and to the magnetometer *RPC-MAG* on the *Orbiter*.

The *Lander* instrumentation has contributions by IWF to the *MUPUS* and *ROMAP* experiments and to the development of the *Rosetta Lander* anchoring system. *MUPUS* consists of a group of sensors to measure the thermal and mechanical properties of layers near the surface. *ROMAP* is a magnetometer to investigate the magnetic field during the descent to the surface and of possible variations after the touchdown.

MIDAS

The dust emitted from the nucleus when solar irradiation becomes strong enough to sublimate the ices is not only creating an essential part of the spectacular coma; it also carries important information on the nucleus. The instrument *MIDAS (Micro-Imaging Dust Analysis System)* aboard the *Rosetta Orbiter* will allow to investigate the texture of individual grains and statistical features of the dust flux by means of atomic force microscopy. The instrument has been developed under the leadership of IWF (see the IWF website for details).

The *MIDAS* FM had been completed and integrated on the *Rosetta Orbiter* in September, 2001. It accompanied the spacecraft during the long series of system level tests in 2002 and 2003, with the exception of July 2003, when the dust collection targets and some of the mechanisms were inspected for any degradation that might have occurred during the extended storage period on the ground (in air).

In preparation of this activity a spare target wheel with specially designed collection surfaces had been prepared. During the inspection the target wheel was indeed exchanged. Finally a software upload was performed, and the instrument was re-integrated. Later on it participated in system functional tests to verify the overall system including instruments, spacecraft and ground segment, and in abbreviated functional tests to check the health of the instrument.

The *MIDAS* team was involved in the preparation of command sequences for the commissioning after launch and in related testing. The *MIDAS* data products for the *Rosetta* archive were defined. Some team members participated in the effort to preserve the knowledge about the experiment throughout the mission and beyond by reporting current knowledge, which is not readily available in written form, on video tape.

In parallel to the flight model activities, the experimental program on the ground continued. The QM of the instrument has served as a test bed for the continuing refinements of the software and for the procedures to be executed during the commissioning phase.

COSIMA

COSIMA (Cometary Secondary Ion Mass Spectrometer) is an instrument on board the *Rosetta Orbiter* dedicated to the chemical and isotopic analysis of dust grains collected in the coma (Fig. 4.12). The work principle is that of secondary ion mass spectrometry (SIMS), when a primary ion beam of high energy is focused to a small spot on the target where it releases molecules out of the target material and ionizes a fraction of 0.1 to 10%. In the case of *COSIMA*, a primary beam of Indium ions at 10 keV is applied. The small spot size of ca. 10 µm radius allows to spatially resolve chemical features on larger single particles. The secondary ions extracted from the target are fed into a time-of-flight mass spectrometer with a large mass range.

Fig. 4.12: The instrument COSIMA with (from left to right) dust inlet, target manipulator unit, primary ion beam system and drift tube for the secondary ion beam.

The development of the instrument is performed by an international collaboration chaired by the Max-Planck-Institut für extraterrestrische Physik (MPE) in Garching, Germany. IWF provides electronics for the primary ion beam system, consisting of high voltage and heater supplies for the ion sources.

In summer 2003, the instrument was removed from the spacecraft, and the ion sources were briefly operated in order to clean them from any contamination that might have occurred during the unforeseen extended storage period on the ground caused by the launch delay. After this successful test, the instrument was re-integrated and later on participated in system functional tests to verify the overall system including instruments, spacecraft and ground segment, and in abbreviated functional tests to check the health of the instrument.

MUPUS

In 2003, the instrument remained integrated in the *Rosetta* spacecraft and participated in system functional tests to verify the overall system including instruments, spacecraft and ground segment, and in abbreviated functional tests to check the health of the instrument.

ROMAP

ROMAP (Rosetta Lander Magnetometer and Plasma Monitor) aboard the *Rosetta Lander* is a multi-sensor experiment. A fluxgate magnetometer (TU Braunschweig) investigates the magnetic field, ion and electron rates are detected by means of an electrostatic analyzer (KFKI Budapest and MPAe Lindau) and the ambient pressure is measured by Pirani and Pennings sensors. The different sensors and their accompanying electronics are controlled by the *ROMAP* controller developed at IWF, which includes the instrument's telemetry interface.

In parallel to *ROMAP*, plasma parameters are measured by the *Rosetta Orbiter*. This makes it possible to investigate the comet-solar wind interaction (generation of the coma and the plasma tail) as function of the distance from the Sun at two different points.

In 2003, the instrument remained integrated in the *Rosetta* spacecraft and participated in system functional tests to verify the overall system including instruments, spacecraft and ground segment, and in abbreviated functional tests to check the health of the instrument.

RPC-MAG

The fluxgate magnetometer *RPC-MAG* is one of the five instruments included in the *Rosetta Plasma Consortium (RPC)*. It is designed to measure the magnetic environment of a comet and to determine its magnetic property. During the two years period of *Rosetta* orbiting around the comet, the comet tail will be observed in detail for the first time. The lead institution of the *RPC-MAG* consortium is the Institut für Geophysik und Meteorologie of TU Braunschweig. The analogue-to-digital converter of the magnetometer is built by IWF.

In 2003, the instrument remained integrated in the *Rosetta* spacecraft and participated in system functional tests to verify the overall system including instruments, spacecraft and ground segment, and in abbreviated functional tests to check the health of the instrument.

5 Laboratory Experiments

The experience of IWF in developing and building instruments for space missions enables the institute to perform laboratory experiments, to develop software and to provide calibration tools for radio antennas.

5.1 Magnetic Cleanliness

In preparation of the *Venus Express* spacecraft (s/c) and its Magnetic Cleanliness, a measurement campaign of the final state of the *Mars Express* s/c was performed at INTESPACE in Toulouse in February 2003 (Fig. 5.1). Since the main instruments on *Venus Express* will be the same as on *Mars Express*, magnetic stray field measurements were made in order to gain better knowledge of their AC and DC fields. Analysis of the stray field data led to magnetic characterization of the different parts, which will allow important improvements in the development of the on-board software (s/w) and the ground-based data calibration s/w for the *Venus Express* magnetic field instrument.

The experience gained in Magnetic Cleanliness expertise, especially through the *Multi-Magnetometer-Sensing* study *(MMS)* finished in 2002, led to contribution in the Magnetic Cleanliness studies and preparations for the *THEMIS* s/c project of NASA. A s/w package, developed for *Rosetta Lander* Magnetic Cleanliness investigations, as well as knowledge and experience of *MMS* for further improvement of this s/w were delivered to UCLA, which is responsible for *THEMIS* Magnetic Cleanliness modeling and calculation.

Fig. 5.1: Mars Express s/c during a measurement campaign at INTESPACE, Toulouse.

5.2 Radio Antennas

Analysis of the Interball 2 antennas: The reception properties of the *POLRAD* antennas of the *Interball 2* satellite were determined by numerical wire-grid calculations, which confirmed earlier rheometric results: The effective axes of the four antennas A1-A4 are tilted by about 6 degrees from their mechanical axes towards antenna A5 (oriented along the spin axis; see Fig. 5.2 when one of the A1-A4 antennas is driven against the spacecraft body and the other antennas are disconnected (i.e. the realistic case of a high impedance between the antennas and the s/c body).

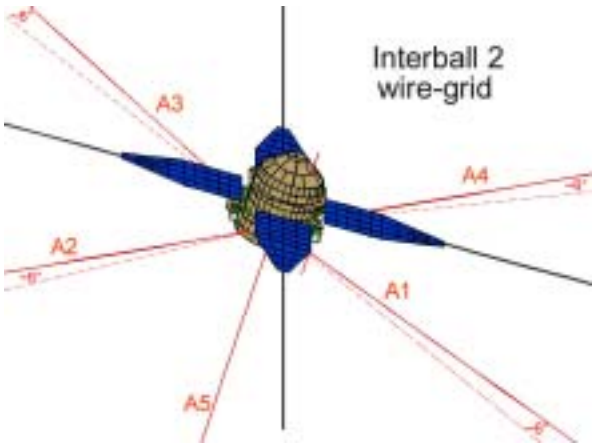

Fig. 5.2: Interball 2 wire-grid model with mechanical antennas and their respective effective height vectors.

Analysis of the MARSIS antenna system: The *MARSIS (Mars Advanced Radar for Subsurface and Ionosphere Sounding)* experiment aboard *Mars Express* is dedicated to the investigation of the Martian surface and ionosphere. It uses a ground penetrating radar to scan the Martian surface and subsurface structure. The primary goal is to map underground water and ice, which is thought to be essential in the search for microbial life on Mars. The *MARSIS* observations will not only give information on the ionosphere and subsurface water- and ice-reservoirs but also on the properties of Martian surface soil layers. In particular, the comparison with findings from planned studies at IWF on Mars soil analogues can give additional clues on soil composition and mechanisms underlying atmosphere-surface interactions.

The *MARSIS* antenna system consists of a primary dipole for transmission and reception of radar pulses, and a secondary receiving monopole for the cancellation of surface clutter echoes. The exact knowledge of the axis of minimum sensitivity of the monopole is decisive for the sounding technique. As the effective axis of the monopole is significantly perturbed by the spacecraft body, the determination of the offset of the axis from the nominal direction is crucial. The monopole radiation pattern is very sensitive to the termination impedances of the dipole and a realistic description of the reception properties of the clutter antenna can only be accomplished by taking into account the impedance matching network of the dipole. We therefore implemented the network in our calculations. Again we based our calculations on a wire-grid model comprising the most important parts of the spacecraft, meanwhile refined (Fig. 5.3).

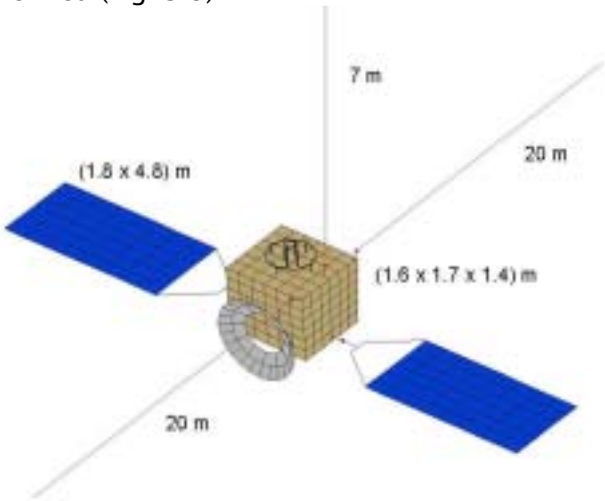

Fig. 5.3: Mars Express wire-grid model with MARSIS antennas.

The new results prove that the network considerably changes the reception properties of the monopole, and that the frequency dependence is dominated by the network. Another aspect, which turned out to be essential, is wave polarization. The polarization of the waves radiated from the dipole, reflected at the Martian surface and returning to the spacecraft is not polarization-matched to the monopole antenna. The polarization match factor varies with direction and has a significant influence on the received voltages. We took this factor into account by establishing the transfer gain, which describes the transfer of power from the transmitting to the receiving antenna and incorporates polarization effects.

A comparison of the monopole transfer gain with the gain of the monopole itself shows that the polarization alters the received signals in a severe way: The monopole gain has a pronounced minimum near nadir, which is deformed by the polarization mismatch into a long valley along the track (see Fig. 5.4).

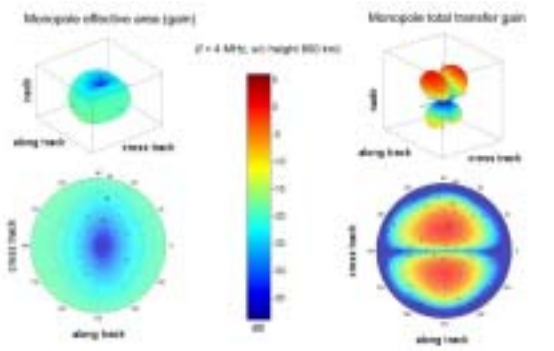

Fig. 5.4: Comparison of monopole gain (left) and total transfer gain (right), representing the power received by the monopole from the return echo. The along-track valley indicates bad polarization matching.

As a result it is questionable if any adjustment of the spacecraft attitude should be performed to point the minimum gain direction towards nadir (as originally planned to improve the clutter cancellation). Instead, we recommend the implementation of refined calibration factors, which are used in the clutter cancellation technique. Corresponding calculations besides some other refinements are in progress.

5.3 Space Simulation

Solid State Greenhouse Effect

The Solid State Greenhouse Effect (SSGE) is an energy transformation process analogous to the well-known atmospheric greenhouse effect: Icy layers are often translucent for radiation in the optical wavelength range. Therefore the energy can be deposited below the surface and this leads to a subsurface temperature increase. The SSGE is expected to play a key role for understanding the thermodynamics of atmosphereless icy bodies in the solar system, like comets and icy satellites. Furthermore, it provides a possible physical mechanism for some enigmatic features observed by the *Mars Global Surveyor* spacecraft at the south polar regions of Mars, the so-called "cryptic regions" and the associated "dark spiders": these are peculiar dark, radially converging dendritic patterns obviously temporarily covered by transparent CO_2 slab ice. The SSGE is investigated theoretically and with the aid of laboratory experiments. The theoretical work consists of two main parts: (a) a thermal model describing the heat transfer, and (b) a model dealing with the radiative transfer problem. The thermodynamic model was developed in order to simulate the behavior of different irradiated transparent ice layers, like dusty H_2O- and CO_2-ice. A typical result of the model calculation showing the temperature increase beneath the surface is given in Fig. 5.5. Since one main input parameter of the thermodynamic model is albedo of the body, another part of the theoretical work deals with the optical properties of different kinds of ice. Simulations were done for porous ices built of Greenberg particles, which consist of a silicate core and an organic shell, and for ices built from irregularly shaped particles of H_2O- and CO_2-ice with embedded spherically shaped dust particles. The basis for calculating the radiative transfer are the wavelength-dependent optical constants of the different particles.

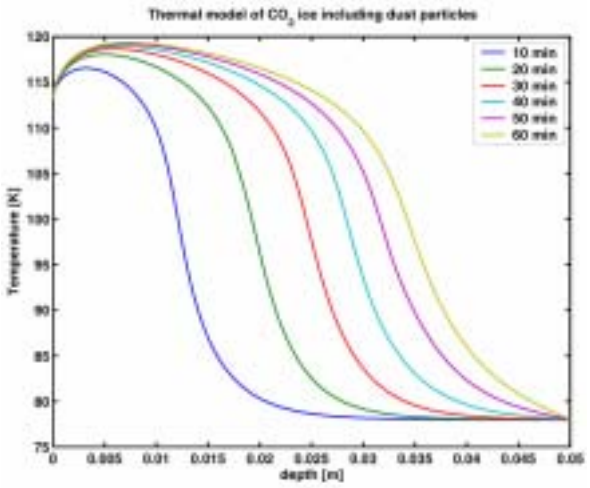

Fig. 5.5: Modelling results for CO_2 slab ice including dust particles: the curves show the temperature distribution inside the ice in response to solar irradiation after 10, 20, 30, 40, 50 and 60 min.

To study the SSGE experimentally, the IWF space simulation chamber had to be adapted. In order to allow for the production of transparent CO_2 slab ice from the gas

phase, a new sample container with a bottom plate cooled by liquid nitrogen was constructed and integrated into the chamber (Fig. 5.6). Also a solar simulator for the irradiation of the ice samples was added.

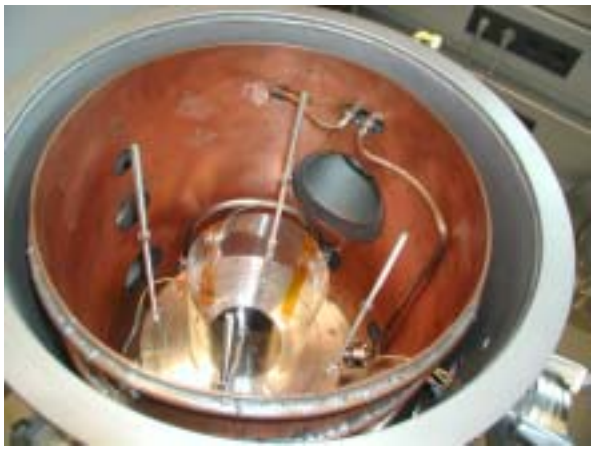

Fig. 5.6: Cooling plate with sample container for the production of transparent CO_2 slab ice.

Exobiology

Several UV exposure experiments on biological samples were conducted in the frame of the ESA Topical Team *ROME (Response of Organism to the Martian Environment)* and the Hungarian exobiology experiment *PUR (Phage and Uracil Response)* carried out in 2004 on ESA's *EXPOSE* facility on board of the *International Space Station*. The focus of the experiments was to simulate UV effects on biological samples of varying doses encountered in different environments, such as in Earth orbit, an O_2- and O_3-free early Earth and at the Martian surface. A variety of Uracil and Phage samples were used for different UV doses, which were generated by a solar simulator and exposed in the IWF space simulation chamber (Fig. 5.7). For the first time a duplicate of *Mars Express' Beagle 2* UV sensor was used directly inside the irradiation chamber alongside the samples, to quantify the UV flux experienced during exposure. This measurement allowed the determination of exposure times for each sample, as a function of wavelength. Another aspect was the use of spare filters, originally produced for *Beagle 2*. These filters allowed selective parts of the UV spectrum to be transmitted to the sample and provide therefore a new measurement of the sole effect of short wavelength UV in narrow band passes. A study is under preparation, which indicates that direct photo-reversion may contribute to the protection of the DNA from UV radiation on planetary surfaces with O_3-free atmospheres.

Fig. 5.7: The solar simulator at the IWF space simulation chamber.

Penetrometry Test Stand

In July 2003 a new project started in continuation of the *NetLander SPICE* instrument work. The main purpose of this project is to establish a model for granular soils on terrestrial planets, e.g. on Mars for ground penetrating instruments.

To maximize the information gained from penetration tests, it is essential to characterize the materials as precise as possible. Therefore the laboratory work is split into two parts. In the first part different materials

are selected and characterized from the geotechnical point of view with standard engineering methods. The most important soil mechanical parameters obtained from penetrometry tests are the shear strength parameters (angle of internal friction and cohesion), the stiffness parameters (Young's modulus and Poisson's ratio), the grain size distribution and the relative density. The best way to determine the shear strength and the stiffness parameters for dry samples is the so-called "triaxial test" (Fig. 5.8, the tests are carried out in cooperation with the Graz University of Technology).

Fig. 5.8: Triaxial test set-up for granular material.

In the second phase penetrometry tests are performed using these well known materials. The aim is to establish a comparison matrix of the soil mechanical parameters and the measured force on the tip of a penetrometer.

The two phases of laboratory work are running in parallel. Thus, it is possible to react on the results of the penetrometry tests, e.g. to use further materials or to determine further parameters.

Vacuum Chamber

For functional tests and calibration of space instruments, including future electron beam experiments, a large vacuum chamber with manipulators and sensors is necessary. A suitable chamber, which had been used for similar purposes, has been received from MPE Garching, Germany. The refurbishment of this chamber has started by adding thermal isolation (Fig. 5.9), the renewal of flanges as necessary, and the replacement of some mechanisms. A new set of vacuum pumps and a new control system will complete this facility, which will allow IWF to proceed with its long-term plans for space instrumentation.

Fig. 5.9: Vacuum chamber with thermal isolation.

A smaller chamber is mainly used for thermal vacuum qualification tests (Fig. 5.10). The achievable temperature ranges between +90 °C and -80 °C. The unit under test is directly mounted to a heat/cold plate and in short distance surrounded by a thermally controlled cylinder. Liquid nitrogen is used for cooling, while high temperatures are achieved by simple electric heating. A dual stage pump system provides the necessary vacuum. The pressure is typically in the range of 2×10^{-6} mbar depending on the temperature and the size of the unit to be tested.

For instruments sensitive to vibration, the vacuum can be maintained by use of an ion getter pump without the use of the dual stage pump. Thermal regulation as well as pump system control is done automatically by a computer, supervised by an independent safety system, which protects the tested unit and vacuum system in case of computer failure or breakdown of mains or water supply.

Fig. 5.10: Thermal Vacuum Test Equipment.

Temperature Test Facility

During space missions, scientific sensors mounted outside of the spacecraft are usually exposed to extreme temperature conditions. This is in particular true for spacecraft of the upcoming ESA missions to Venus (*Venus Express*, launch 2005) and Mercury (*BepiColombo*, launch 2012).

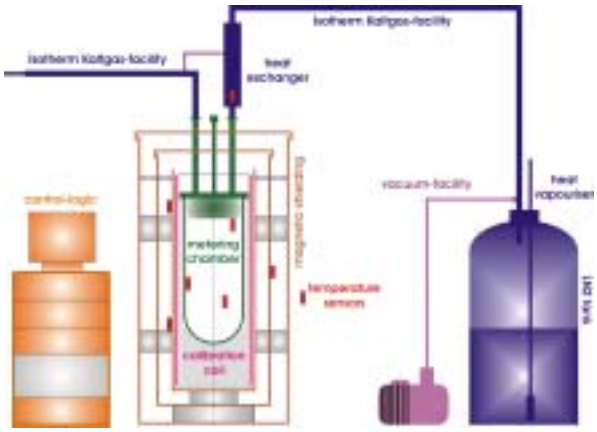

Fig. 5.11: Temperature test facility for magnetic field sensors.

For this reason a special temperature test facility (Fig. 5.11) for magnetic field sensors was constructed which consists of a three layer magnetic shielding set, temperature control equipment and a calibration coil for magnetic field stimuli and allows all basic test and calibration measurements (offset, scale factor, transfer function, etc.) especially for magnetic field sensors between −170 °C and +200 °C, controlled to a precision of 0.1 °C.

In 2003, the qualification (EQM) as well as the first flight model (FM-1) of the *Double Star* magnetometer *(FGM)* have successfully been calibrated and tested using this facility.

5.4 COROT

In co-operation with the Institute for Astronomy, University of Vienna, IWF contributes to the French space telescope *COROT (Convection, Rotation and Planetary Transit)*. The scientific goal is the investigation of dynamic processes in the interior of stars and the search and survey of extrasolar planets. In both cases, astroseismology and exoplanetology, the variation of the brightness of stars is the key parameter. The determination of these variations is done by high precision photometry, with a resolution better than 10 ppm. In astroseismology, the amplitude and frequency of brightness variations is used to derive the oscillation mode and furthermore to determine the physical and chemical processes in the interior. Variations in the brightness can be caused by bypassing planets, too. Therefore, this effect is used to identify extrasolar planets. To distinguish variation due to oscillations from bypassing planets, spectral analysis in the red and blue zone is performed. In astroseismology, only a few targets are observed, while in exoplanetology the data of 6000 stars are processed simultaneously.

IWF develops the so-called extractor *(Boîtiers Extracteur, BEX)* a computer system with dedicated pre-processors for the selection and classification of image data. The in-house developed pre-processors allow the identification of pixels, which are part of pre-defined image areas, up to a data rate of 200 kpixel/s. The essential technology is hardware supported data mining under the constraints for real-time operation. In addi-

tion to the development and assembly of the space-qualified hard- and software as well as the ground support equipment, IWF will participate in the integration and test campaign.

The pre-defined image areas are irregular patterns, which compensate the non-linearity of the optics. The processor load is directly depending on the position of the pre-defined areas; therefore, clustering shall be avoided. The so-called look-up table generator program supports the placement, creates the look-up table and estimates the needed system performance.

Fig. 5.12: Laboratory model of BEX.

The existing design for the laboratory model (Fig. 5.12) was transferred into the final one used for engineering and flight models. A first version of the software, providing the basic functionality was developed and tested. Presently, the team concentrates on the manufacturing of the engineering model.

Exoplanetary atmospheric loss: Past studies addressing thermal atmospheric escape of hydrogen from short periodic giant exoplanets have been based on the planet's effective temperature, which however is not physically relevant for atmospheric loss processes. In consequence, these studies led to significant underestimations of atmospheric escape rates and to the conclusion of long-term atmospheric stability. From more realistic exospheric temperatures, determined from XUV irradiation and thermal conduction in the thermosphere of such planets, we found that hydrodynamic conditions occur so that energy-limited escape and atmospheric expansion up to 3 planetary radii arise, leading to much higher estimations for hydrogen loss rates in the order of about 5×10^{11} gs^{-1}.

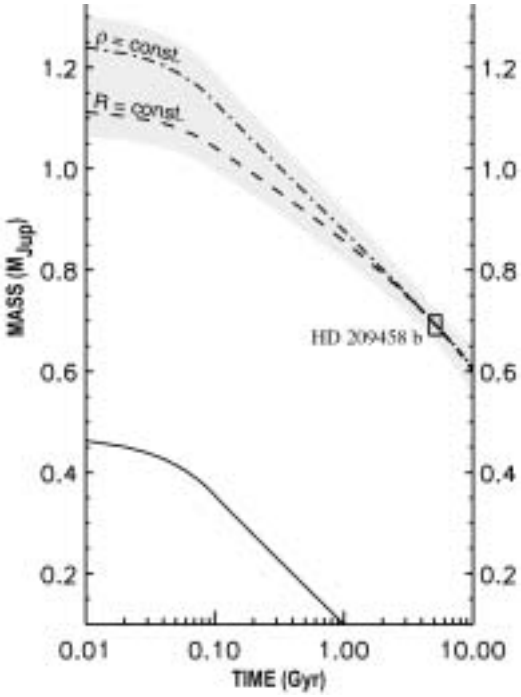

Fig. 5.13: Long term evolution of the mass of HD 209458b from XUV-driven thermal escape. The shaded area represents the envelope of evolution scenarios. The solid curve shows the evolution of a gaseous planet at the same orbital, which fully evaporates after 1 Gyr.

The calculated loss rates are in good agreement with recent determinations for the Jovian-like exoplanet HD 209458b based on observations of its extended exosphere of about 2.7 planetary radii and a lower hydrogen loss rate of about $>10^{10}$ gs^{-1}. The IWF study suggests that for young solar-type stars, which emit stronger XUV fluxes, the inferred loss rates are significantly higher. By simulating the atmospheric evolution of hydrogen-rich giant exoplanets under such strong XUV irradiances we found as shown in Fig. 5.13 that giant exoplanets may evaporate down to their core sizes or shrink to levels where heavier atmospheric constituents may prevent hydro-dynamic conditions.

The study of the exospheric environment of short-periodic exoplanets under hydrodynamic conditions with the support of transit data by *COROT* will open a unique opportunity in the understanding of the effect of hydrodynamic escape.

6 Publications & Talks

6.1 Refereed Articles

Arsov, K., R. Pail: Assessment of two methods for gravity field recovery from GOCE GPS-SST orbit solutions, *Adv. Geosci.*, **1**, 121-126 (2003)

Asano, Y., T. Mukai, M. Hoshino, Y. Saito, H. Hayakawa, T. Nagai: Evolution of the thin current sheet in a substorm observed by Geotail, *J. Geophys. Res.*, **108**, doi:10.1029/2002JA009785 (2003)

Becker, R.H., R.N. Clayton, E.M. Galimov, H. Lammer, B. Marty, R.O. Pepin, R. Wieler: Isotopic Signatures of Volatiles in Terrestrial Planets, *Space Sci. Rev.*, **106**, 377-410 (2003)

Ellery, A., C. Kolb, H. Lammer, J. Parnell, H. Edwards, L. Richter, M.R. Patel, J. Romstedt, D. Dickensheets, A. Steele, C. Cockell: Astrobiological Instrumentation for Mars - The Only Way is Down, *Int. J. Astrobiol.*, **1**, 365-380 (2003)

Erkaev, N.V., C.J. Farrugia, H.K. Biernat: The role of the magnetic barrier in the solar wind-magnetosphere interaction, *Planet. Space Sci.*, **51**, 745-755 (2003)

Gubchenko, V.M., H.K. Biernat, M. Goossens: On the quasi-current-free electrodynamics of current-carrying hot space plasma, *Adv. Space Res.*, **31**, 1277-1283 (2003)

Gumbel, J., D.E. Siskind, G. Witt, K.M. Torkar, M. Friedrich: Influences of ice particles on the ion chemistry of the polar summer mesosphere, *J. Geophys. Res.*, **108**, doi:10.1029/2002JD002413 (2003)

Johannessen, J.A., G. Balmino, C. Le Provost, R. Rummel, R. Sabadini, H. Sünkel, C.C. Tscherning, P. Visser, P. Woodworth, C. Hughes, P. Legrand, N. Sneeuw, F. Perosanz, M. Aguirre-Martinez, H. Rebhan, M. Drinkwater: The European Gravity Field and Steady-State Ocean Circulation Explorer Satellite Mission: Its Impacton Geophysics, *Surv. Geophys.*, **24**, 339-386 (2003)

Kallenbach, R., F. Robert, J. Geiss, E. Herbst, H. Lammer, B. Marty, T.J. Millar, U. Ott, R.O. Pepin: Sun and Protosolar Nebula, *Space Sci. Rev.*, **106**, 319-376 (2003)

Khodachenko, M.L., G. Haerendel, H.O. Rucker: Inductive electromagnetic effects in solar current-carrying magnetic loops, *Astron. & Astrophys.*, **401**, 721-732 (2003)

Lammer, H., C. Kolb, T. Penz, U.V. Amerstorfer, H.K. Biernat, B. Bodiselitsch: Estimation of the past and present Martian water-ice reservoirs by isotopic constraints on exchange between the atmosphere and the surface, *Int. J. Astrobiol.*, **2**, 195-202 (2003)

Lammer, H., F. Selsis, I. Ribas, E.F. Guinan, S.J. Bauer, W.W. Weiss: Atmospheric Loss of Exoplanets Resulting from Stellar X-Ray and Extreme-Ultraviolet Heating, *Astrophys. J. Lett.*, **598**, L121-L124 (2003)

Lammer, H., H.I.M. Lichtenegger, C. Kolb, I. Ribas, E.F. Guinan, R. Abart, S.J. Bauer: Loss of water from Mars: Implications for the oxidation of the soil, *Icarus*, **165**, 9-25 (2003)

Lammer, H., P. Wurz, M.R. Patel, R. Killen, C. Kolb, S. Massetti, S. Orsini, A. Milillo: The variability of Mercury`s exosphere by particle and radiation induced surface release processes, *Icarus*, **166**, 238-247 (2003)

Lammer, H., S.J. Bauer: Isotopic fractionation by gravitational escape, *Space Sci. Rev.*, **106**, 281-291 (2003)

Leubner, M.P.: An analytical representation of non-gyrotropic distributions and related space applications, *Planet. Space Sci.*, **51**, 723-729 (2003)

Leubner, M.P.: Wave induced energetic particle generation and space plasma modeling, *Space Sci. Rev.*, **107**, 361–368 (2003)

Magnes, W., D. Pierce, A. Valavanoglou, J. Means, W. Baumjohann, C.T. Russell, K. Schwingenschuh, G. Graber: A sigma-delta fluxgate magnetometer for space applications, *Meas. Sci. Technol.*, **14**, 1003–1012 (2003)

Massetti, S., S. Orsini, A. Milillo, A. Mura, E. De Angelis, H. Lammer, P. Wurz: Mapping of the cusp plasma precipitation on the surface of Mercury, *Icarus*, **166**, 229–237 (2003)

Matsui, H., J.M. Quinn, R.B. Torbert, V.K. Jordanova, W. Baumjohann, P.A. Puhl-Quinn, G. Paschmann: Electric field measurements in the inner magnetosphere by Cluster EDI, *J. Geophys. Res.*, **108**, doi:10.1029/2003JA009913 (2003)

Morente, J.A., G.J. Molina-Cuberos, J.A. Portí, B.P. Besser, A. Salinas, K. Schwingenschuh, H.I.M. Lichtenegger: A numerical simulation of Earth's electromagnetic cavity with the Transmission Line Matrix method: Schumann resonances, *J. Geophys. Res.*, **108**, doi:10.1029/2002JA009779 (2003)

Morente, J.A., G.J. Molina-Cuberos, J.A. Portí, K. Schwingenschuh, B.P. Besser: A study of the propagation of electromagnetic waves in Titan's atmosphere with the TLM numerical method, *Icarus*, **162**, 374–384 (2003)

Mühlbachler, S., C.J. Farrugia, H.K. Biernat, R.B. Torbert: The geostationary field during dayside erosion events 1996–2001: A joint WIND, ACE, and GOES study, *J. Geophys. Res.*, **108**, doi: 10.1029/2003JA009833 (2003)

Mühlbachler, S., V.V. Ivanova, V.S. Semenov, H.K. Biernat, D. Langmayr, D.F. Vogl: Time-dependent reconnection for anisotropic pressure, *Phys. Plasmas*, **10**, 655–663 (2003)

Nagai, T., I. Shinohara, M. Fujimoto, S. Machida, R. Nakamura, Y. Saito, T. Mukai: Structure of the Hall current system in the vicinity of the magnetic reconnection site, *J. Geophys. Res.*, **108**, doi:10.1029/2003JA009900 (2003)

Nickolaenko, A.P., B.P. Besser, K. Schwingenschuh: Model computations of Schumann resonance on Titan, *Planet. Space Sci.*, **51**, 853–862 (2003)

Noda, H., W. Baumjohann, R. Nakamura, K.M. Torkar, G. Paschmann, H. Vaith, P. Puhl-Quinn, M. Förster, R. Torbert, J.M. Quinn: Tail lobe convection observed by Cluster/EDI, *J. Geophys. Res.*, **108**, doi:10.1029/2002JA009669 (2003)

Patel, M.R., A. Bercés, C. Kolb, H. Lammer, P. Rettberg, J.C. Zarnecki, F. Selsis: Seasonal and diurnal variations in Martian surface UV irradiation: Biological and chemical implications for the Martian regolith, *Int. J. Astrobiol.*, **2**, 21–34 (2003)

Petrukovich, A.A., W. Baumjohann, R. Nakamura, A. Balogh, T. Mukai, K.-H. Glaßmeier, H. Rème, B. Klecker: Plasma sheet structure during strongly northward IMF, *J. Geophys. Res.*, **108**, doi:10.1029/2002JA009738 (2003)

Rontó, G., A. Bercés, H. Lammer, C.S. Cockell, G.J. Molina-Cuberos, M.R. Patel, F. Selsis: Solar UV irradiation conditions on the surface of Mars, *Photochem. Photobiol.*, **77**, 34–40 (2003)

Runov, A.V., R. Nakamura, W. Baumjohann, R.A. Treumann, T.L. Zhang, M. Volwerk, Z. Vörös, A. Balogh, K.-H. Glaßmeier, B. Klecker, H. Rème, L. Kistler: Current sheet structure near magnetic X-line observed by Cluster, *Geophys. Res. Lett.*, **30**, doi:10.1029/2002GL016730 (2003)

Runov, A.V., R. Nakamura, W. Baumjohann, T.L. Zhang, M. Volwerk, H.-U. Eichelberger, A. Balogh: Cluster observation of a bifurcated current sheet, *Geophys. Res. Lett.*, **30**, doi: 10.1029/2002GL016136 (2003)

Sergeev, V., A.V. Runov, W. Baumjohann, R. Nakamura, T.L. Zhang, M. Volwerk, A. Balogh, H. Rème, J.A. Sauvaud, M. André, B. Klecker: Current sheet flapping motion and structure observed by Cluster, *Geophys. Res. Lett.*, **30**, doi:10.1029/2002GL016500 (2003)

Shi, J.K., B.Y. Xu, K. Torkar, T.L. Zhang, Z.X. Liu: An electrostatic model for nonlinear waves in the upper ionosphere, *Adv. Space Res.*, **32**, 303–308 (2003)

Shiokawa, K., W. Baumjohann, G. Paschmann: Bidirectional electrons in the near-Earth plasma sheet, *Ann. Geophys.*, **21**, 1497–1507 (2003)

Vogl, D.F., D. Langmayr, H.K. Biernat, N.V. Erkaev, C.J. Farrugia, S. Mühlbachler: The solution of

the Rankine-Hugoniot equations for fast shocks in an anisotropic kappa distributed medium, *Planet. Space Sci.*, **51**, 715-722 (2003)

Vogl, D.F., D. Langmayr, H.K. Biernat, N.V. Erkaev, S. Mühlbachler: The anisotropic jump equations for oblique fast shocks in a kappa distributed medium, *Adv. Space Res.*, **32**, 519-523 (2003)

Volkonskaya, N.N., T.N. Volkonskaya, V.S. Semenov, H.K. Biernat: Energy and momentum balance of time-dependent magnetic Petschek-type reconnection, *Int. J. Geomag. Aeron.*, **3**, 245-253 (2003)

Volwerk, M., K.-H. Glaßmeier, A.V. Runov, W. Baumjohann, R. Nakamura, T.L. Zhang, B. Klecker, A. Balogh, H. Rème: Kink mode oscillation of the current sheet, *Geophys. Res. Lett.*, **30**, doi:10.1029/2002GL016467 (2003)

Volwerk, M., R. Nakamura, W. Baumjohann, R.A. Treumann, A.V. Runov, Z. Vörös, T.L. Zhang, Y. Asano, B. Klecker, I. Richter, A. Balogh, H. Rème: A statistical study of compressional waves in the tail current sheet, *J. Geophys. Res.*, **108**, doi:10.1029/2003JA010155 (2003)

Vörös, Z., W. Baumjohann, R. Nakamura, A. Runov, T.L. Zhang, M. Volwerk, H.U. Eichelberger, A. Balogh, T.S. Horbury, K.-H. Glaßmeier, B. Klecker, H. Rème: Multi-scale magnetic field intermittence in the plasma sheet, *Ann. Geophys.*, **21**, 1955-1964 (2003)

Wurz, P., H. Lammer: Monte-Carlo simulation of Mercury's exosphere, *Icarus*, **164**, 1-13 (2003)

Zaitsev, V.V., V.E. Shaposhnikov, H.O. Rucker: Electron acceleration in the ionosphere of Io, *Astron. Rep.*, **47**, 701-708 (2003)

Zaitseva, S.A., S.N. Akhremtchik, M.I. Pudovkin, Ya.V. Galtsova, B.P. Besser, R.P. Rijnbeek: Long-term variations of the solar activity-lower atmosphere relationship, *Int. J. Geomag. Aeron.*, **4**, 167-174 (2003)

6.2 Proceedings and Book Chapters

Becker, R.H., R.N. Clayton, E.M. Galimov, H. Lammer, B. Marty, R.O. Pepin, R. Weiler: Isotopic Signatures of Volatiles in Terrestrial Planets. In: *Solar System History from Isotopic Signatures of Volatile Elements*, Eds. R. Kallenbach et al., Kluwer, Dordrecht, 377-410 (2003)

Harrich, M., M. Friedrich, S.R. Marple, K.M. Torkar: The background absorption at high latitudes, *Adv. Rad. Sci.*, **1**, 325-327 (2003)

Kallenbach, R., F. Robert, J. Geiss, E. Herbst, H. Lammer, B. Marty, T.J. Millar, U. Ott, R.O. Pepin: Sun and Protosolar Nebula. In: *Solar System History from Isotopic Signatures of Volatile Elements*, Eds. R. Kallenbach et al., Kluwer, Dordrecht, 319-377 (2003)

Kolb, C., R. Abart, E. Wappis, T. Penz, E.K. Jessberger, H. Lammer: The Meteoritic Component on the Surface of Mars: Implications for Organic and Inorganic Geochemistry, *Meteoritics & Planetary Sci., Supplement*, **38**, A15 (2003)

Kolb, C., R. Abart, G. Raggl, P. Ulmer, W. Lottermoser: Synthetic Mars Analogue Materials, *Mitt. Österr. Miner. Ges.*, **148**, 192-193 (2003)

Kolb, C., R. Abart, R. Kaindl: Regolith Mixing Relationships on the Surface of Mars: Influence on Mineralogy and Geochemistry, *Mitt. Österr. Miner. Ges.*, **148**, 189-191 (2003)

Lammer, H., S.J. Bauer: Isotopic fractionation by gravitational escape. In: *Solar System History from Isotopic Signatures of Volatile Elements*, Eds. R. Kallenbach et al., Kluwer, Dordrecht, 281-292 (2003)

Pesec, P., G. Stangl: Structuring CERGOP information, *Rep. Geodesy*, **64**, 23-28 (2003)

Pesec, P., I. Fejes: CERGOP-2/Environment - A challenge for the next 3 years, *Rep. Geodesy*, **64**, 13-22 (2003)

Stangl, G.: Deficits of CEGRN solution and time series, *Rep. Geodesy*, **64**, 29-32 (2003)

Thiel, M., J. Stöcker, C. Rohe, N.I. Kömle, G. Kargl, O. Hillenmaier, P. Lell: The ROSETTA Lander Anchoring System. In: *Proc. 10th European Space Mechanisms and Tribology Symposium*, Ed. R.A. Harris, ESA SP-524, 239-246 (2003)

Vörös, Z., L. Pastorek, I. Dorotovic: Multi-scale aspects of solar cycle variability. In: *Solar Variability as an Input to the Earths Environment*, Ed. A. Wilson, ESA SP-535, 173-175 (2003)

6.3 Books

Chian, A.C.-L., I.H. Cairns, S.B. Gabriel, J.P. Goedbloed, T. Hada, M. Leubner, L. Nocera, R. Stening, F. Toffoletto, C. Uberoi, J.A. Valdivia, U. Vill (Eds.): Advances in Space Environment Research - Volume I, Kluwer, Dordrecht, 540 pages (2003)

6.4 Other Publications

Aydogar, Ö.: Fluxgate Magnetometer Offset Calibration for DoubleStar FGM, FM1, IWF 2003/03, 6 pages (2003)

Badura, T. Klostius, R. Arsov, K.: ASAP Project - GOCE DAPC Graz - Phase 1a WP Ia-4.2: Core Solver SST, Final Report, 39 pages (2003)

Besser, B.P.: Pioneers from other German speaking countries - Austria, IAC Technical Paper IAC-03-IAA.2.4.b.02, 6 pages (2003)

Boudjada, M.Y., A. Stangl, S. Sawas, H.O. Rucker, and the INTAS project teams: Catalogue of the C3-Solar campaign (29th April 2001 to 20th June 2001) at the Kharkov radio station, IWF 148, 70 pages (2003)

Boudjada, M.Y., J. Pickett: Wide Band Data (WBD) Plasma Wave Experiment on board CLUSTER satellites: Selected events of radio wave structures observed close to the Earth's magnetic equatorial regions, IWF 147, 24 pages (2003)

Eichelberger, H.-U. et al.: Double Star FGM EQM Sample Rate and Frequency Response Analysis, IWF 2003/01, 29 pages (2003)

Eichelberger, H.-U. et al.: DoubleStar FGM FM1 Sample Rate and Frequency Response Analysis, IWF 2003/02, 39 pages (2003)

Jaritz, G.F., H.K. Biernat, N.V. Erkaev, R.A. Treumann, D.F. Vogl, C.J. Farrugia, D. Langmayr, S. Mühlbachler: Anisotropic fast shocks: Application to the Earth's bow shock, 151, 69 pages (2003)

Leitner, M., H.K. Biernat, C.J. Farrugia, S. Mühlbachler, D. Langmayr, D.F. Vogl: The sheath region of interplanetary magnetic clouds modelled as force-free cylindrical magnetic flux ropes: HELIOS and WIND observations, IWF 150, 91 pages (2003)

Macher, W., T. Vejda: Design of antenna grid structures, IWF 144, 103 pages (2003)

Metzler, B., F. Weimann: GOCE DAPC Graz, Phase Ia, Workpackage Ia-4.4, Final Report, 28 pages (2003)

Penz, T., H.K. Biernat, H. Lammer, N.V. Erkaev, I.L. Arshukova, U.V. Amerstorfer: Planetary ion loss due to magnetohydrodynamic instabilities, IWF 149, 96 pages (2003)

Penz, T., H.K. Biernat, V.S. Semenov, N.V. Erkaev, I.V. Kubyshkin, I.V. Alexeev, N.N. Volkonskaya, S. Mühlbachler: A theoretical model for the reconstruction of reconnection structures from satellite measurements, IWF 149, 96 pages (2003)

Pesec, P.: Semi-annual report for CERGOP-2/Environment, Semi-annual report for EU, 9 pages (2003)

Sawas, S., M.Y. Boudjada, A. Lecacheux, A. Stangl, H.O. Rucker, W. Voller: Interactive Software for Spectral Analysis (ISSA), IWF 141, 47 pages (2003)

Vejda, T., W. Macher, G. Fischer, M.Y. Boudjada, H.O. Rucker: Solar orbiter wire grid model, IWF 145, 20 pages (2003)

6.5 Invited Talks

Baumjohann, W.: Bifurcated magnetotail current sheets, *IUGG Assembly*, Sapporo, Jul 2003.

Baumjohann, W.: Das Institut für Weltraumforschung, *APART-Symposium*, Vienna, Apr 2003.

Baumjohann, W.: SCOSTEP's CAWSES programme, *E-STAR Science Meeting*, Illkirch, Nov 2003.

Baumjohann, W.: The view of European space policy from science, *Green Paper European Space Policy Information Panel*, Vienna, May 2003.

Besser, B.P.: Pioneers from other German speaking countries: Austria, *IAC*, Bremen, Sep 2003.

Lammer, H., et al.: Atmospheric evolution of exoplanets due to thermal and non-thermal loss processes, *Light on Planetary Atmospheres*, University of Amsterdam, Dec 2003.

Leubner, M.P.: Fundamental gravitational entropy constraints as source of global cosmic inho-

mogeneity scales, *10th Marcel Grossmann Conference*, Rio de Janeiro, Jul 2003.

Leubner, M.P.: Fundamental issues on kappa-distributions in space plasmas, *EGS-AGU-EUG Joint Assembly*, Nice, Apr 2003.

Nakamura, R., et al.: Cluster multi-point observations of fast flows in the plasma sheet, *IUGG Assembly*, Sapporo, Jul 2003.

Nakamura, R., et al.: Cluster multi-point observations of the flow and field disturbances in the central plasma sheet, *EGS-AGU-EUG Joint Assembly*, Nice, Apr 2003.

Nakamura, R.: Magnetotail Transport Process and Space Weather, *Geomagnetic Field and Space Weather Symposium*, Potsdam, May 2003.

Rucker, H.O.: Fundamental Jupiter millisecond radio burst characteristics, *EGS-AGU-EUG Joint Assembly*, Nice, Apr 2003.

Runov, A.V., et al.: Cluster multi-point observations of the magnetotail current sheet structure and dynamics, *STAMMS Conference*, Orléans, May 2003.

Torkar, K.M.: MIDAS - an Atomic Force Microscope for Cometary Dust Samples, *Workshop "Nanotechnology in Space"*, Munich, Oct 2003.

Torkar, K.M.: The Double Star Data System, *Cluster Workshop*, ESTEC, Oct 2003.

6.6 Oral Presentations

Arsov, K.: Graz GOCE group activities and processing techniques development in view of the long wavelength gravity field information recovery from the orbit information of the European GOCE mission, *1st Workshop on Int. Gravity Field Res.*, Graz, May 2003.

Baumjohann, W., R.A. Treumann: The role of the Hall effect in tail reconnection, *Cluster Tail Workshop*, Graz, Mar 2003.

Baumjohann, W., T.L. Zhang: Magnetic field investigation of the Venus plasma environment: What do we expect from the Venus Express mission, *IUGG Assembly*, Sapporo, Jul 2003.

Besser, B.P., et al.: Schumann resonances in the atmosphere of Titan, *Jahrestagung der Astronomischen Gesellschaft*, Freiburg, Sep 2003.

Biernat, H.K., et al.: MHD effects as a consequence of the solar wind surrounding Venus and Mars, *26th Ann. Seminar*, Apatity, Jan 2003.

Biernat, H.K.: Institutsstruktur, wiss. Arbeiten der Abt. für exp. Weltraumforschung, Physik d. erdnahen Weltraums: Solar-Planetare Beziehungen, Polar Geophysical Institute, Murmansk, Feb 2003.

Cristea, E., P. Pesec: Use of permanent GPS networks in geodynamics and disaster reduction, *Regional Workshop on the Use of Space Technology for Disaster Management for Europe*, Poiana Brasov, May 2003.

Delva, M., H. Feldhofer, K. Schwingenschuh, K. Mehlem: Multiple magnetic sensor technique for field measurements in space, *EGS-AGU-EUG Joint Assembly*, Nice, Apr 2003.

Kargl, G.: Space simulation facilities at the IWF Graz, The Open University, PSSRI, PSSRI, Open University, Milton-Keynes, Jun 2003.

Kazeminejad, B., D.H. Atkinson: The ESA Huygens Probe Entry and Descent Trajectory Reconstruction, *Int. Workshop on Planetary Probe Atmospheric Entry and Descent Trajectory Analysis and Science*, Lisbon, Oct 2003.

Khodachenko, M.L., H.O. Rucker: Theoretical models of solar dynamic phenomena for STEREO/WAVES, University of California, Berkeley, Dec 2003.

Khodachenko, M.L., T.D. Arber, A. Hanslmeier, H.O. Rucker: Comparative analysis of collisional and viscous damping of MHD waves in the partially ionized solar plasmas, *1st Central European Solar Physics Meeting*, Bairisch Kölldorf, Oct 2003.

Kirchner, G., F. Koidl: kHz SLR at Graz: Now operational, ILRS Workshop, Kötzting, Oct 2003.

Kolb, C., R. Abart, R. Kaindl: Regolith Mixing Relationships on the Surface of Mars: Influence on Mineralogy and Geochemistry, *MinPet*, Neukirchen, Sep 2003.

Kolb, C., R. Abart: Oxidationsexperimente unter Marsbedingungen, Fritz-Haber-Institut, Berlin, Jan 2003.

Kömle, N.I.: Eis und Wasser am Mars: jetzt und früher? Astronomische Vereinigung Kärntens, Klagenfurt, Dec 2003.

Kömle, N.I.: In situ exploration of a comet: Rosetta and Rosetta Lander, Beijing University, Oct 2003.

Lammer, H., A. Hanslmeier, I. Ribas, F. Selsis, E.F. Guinan: The radiation and particle environment of the young Sun and its influence on planetary environments, *1st Central European Solar Physics Meeting*, Bairisch Kölldorf, Oct 2003.

Lammer, H., F. Selsis, C. Kolb, H.I.M. Lichtenegger, I. Ribas, E.F. Guinan, S.J. Bauer: Evolution of the Martian water inventory, *EGS-AGU-EUG Joint Assembly*, Nice, Apr 2003.

Lammer, H., F. Selsis, I. Ribas, E.F. Guinan, S.J. Bauer, W.W. Weiss: Thermal loss in exosolar planetary atmospheres, *EGS-AGU-EUG Joint Assembly*, Nice, Apr 2003.

Lammer, H., et al.: COROT's role in the first detection of hot Neptune-class exoplanets, *4th COROT Week*, Marseille, Jun 2003.

Lammer, H., H.I.M. Lichtenegger, S.J. Bauer: Hot atomic hydrogen and its influence on the exosphere temperature on Venus and Mars, *EGS-AGU-EUG Joint Assembly*, Nice, Apr 2003.

Lammer, H., H.K. Biernat, D.F. Vogl: Radiation and plasma heating of upper planetary atmospheres, *26th Ann. Seminar*, Apatity, Feb 2003.

Lammer, H., T. Penz, H.K. Biernat, A. Stadelmann, J.-M. Grießmeier, F. Selsis: Stellar planetary relations: Characterization of small extrasolar planets detectable by CoRoT, *5th COROT Week*, Berlin, Dec 2003.

Lammer, H.: Atmospheric evolution of exoplanets due to thermal and non-thermal loss processes, TU Braunschweig, Nov 2003.

Lammer, H.: Estimation of the present and past Martian water-ice reservoirs due to D/H isotope ratios, British Antarctic Survey, Cambridge, Sep 2003.

Lammer, H.: Estimation of the present and past water-ice reservoirs on Mars by constraints on exchange between the atmosphere and the surface, *3rd European Workshop on Exo/Astrobiology*, Madrid, Nov 2003.

Lammer, H.: Wiss. Arbeiten der Abt. für Physik des erdnahen Weltraums: Planetare Atmosphären, Oberflächen von Objekten im Sonnensystem, Polar Geophysical Institute, Murmansk, Feb 2003.

Langmayr, D., N.V. Erkaev, H.K. Biernat, H.O. Rucker, S. Mühlbachler, D.F. Vogl: Slow mode wave progagation in a magnetic field, *26th Ann. Seminar*, Apatity, Feb 2003.

Mühlbachler, S., C.J. Farrugia, H.K. Biernat, V.S. Semenov, D.F. Vogl, D. Langmayr: Erosion at geostationary orbit: a statistical study between 1996-2001, *26th Ann. Seminar*, Apatity, Feb 2003.

Mühlbachler, S., C.J. Farrugia, H.K. Biernat, V.S. Semenov, N.V. Erkaev, D.F. Vogl, D. Langmayr: Dayside magnetosphere erosion, *EGS-AGU-EUG Joint Assembly*, Nice, Apr 2003.

Mühlbachler, S.: Dayside magnetosphere erosion, Max-Planck Institut für Aeronomie, Katlenburg-Lindau, Nov 2003.

Mühlbachler, S.: Solar-Wind Magnetosphere Interaction, Queen Mary Coll., London, Nov 2003.

Nakamura, R., et al.: Fast flow during current sheet thinning, *Cluster Tail Workshop*, Graz, Mar 2003.

Nakamura, R., et al.: Field aligned current observed by Cluster and Geotail, *Cluster Tail Workshop*, Graz, Mar 2003.

Nakamura, R., et al.: Plasma sheet expansion and plasma sheet flows, *Cluster Tail Workshop*, Graz, Mar 2003.

Nakamura, R., et al.: Cluster multi-point observations of plasma sheet fast flow structure, *STAMMS Conference*, Orléans, May 2003.

Nakamura, R.: Cluster magnetotail investigations, Mullard Space Science Laboratory, Dorking, Oct 2003.

Pesec, P., et al.: CERGOP-2/Environment - a challenging task for 3 years, *IUGG Assembly*, Sapporo, Jul 2003.

Pesec, P., et al.: EUREF and CERGOP-2, a cooperative task for the next 5 years? *EUREF Symposium 2003*, Toledo, Jun 2003.

Pesec, P.: The use of GPS and Laser for geodynamical investigations in the East Alpine Area, Romanian Academy of Technical Sciences, Bukarest, Nov 2003.

Rucker, H.O., et al.: Determination of effective antenna vectors: From Interball, Mars Express and Cassini to the STEREO Mission, University of California, Berkeley, Dec 2003.

Runov, A.V., et al.: Reconstructions of the magnetotail current sheet structure using four-point Cluster measurements, *Magnetospheric Response to Solar Activity*, Prague, Sep 2003.

Runov, A.V.: Magnetic reconnection in the magnetotail: In situ Cluster multipoint observations, *AGU Fall Meeting*, San Francisco, Dec 2003.

Runov, A.V., et al.: Bifurcated current sheet, *Cluster Tail Workshop*, Graz, Mar 2003.

Runov, A.V., et al.: Current sheet near X-line, *Cluster Tail Workshop*, Graz, Mar 2003.

Runov, A.V., et al.: 3-D structure of a reconnection region observed by Cluster on 1 October 2001, *EGS-AGU-EUG Joint Assembly*, Nice, Apr 2003.

Runov, A.V., et al.: Cluster observation of a reconnection region in the magnetotail plasma sheet, *IUGG Assembly*, Sapporo, Jul 2003.

Stangl, G., E. Cristea: Report on the OLG LAC EPN and other activities, *EUREF Workshop*, Graz, Sep 2003.

Torkar, K.M., M. André, A. Fazakerley: Modelling requirements related to spacecraft potential control by an ion gun, *4th SPINE Workshop*, Noordwijk, Feb 2003.

Torkar, K.M., et al.: The MIDAS atomic force microscope for cometary dust: technical highlights and future perspectives, *EGS-AGU-EUG Joint Assembly*, Nice, Apr 2003.

Torkar, K.M.: Cluster results on ion emitter operation, *5th SPINE Workshop*, Noordwijk, Sep 2003.

Torkar, K.M.: Spurengase und ihre Auswirkung auf die Funkwellenausbreitung, *7. Europäischer Chemielehrerkongress*, Linz, Apr 2003.

Vogl, D.F., M. Leubner, H.K. Biernat, N.V. Erkaev: Cyclotron and mirror modes at a perpendicular fast shock for anisotropic plasma conditions, *EGS-AGU-EUG Joint Assembly*, Nice, Apr 2003.

Vogl, D.F.: Planetary Radio Emissions in Graz, Polar Geophysical Institute, Murmansk, Feb 2003.

Vogl, D.F.: Plasma and field parameters across fast shocks in a kappa distributed medium, Observatoire de Paris Meudon, Paris Meudon, Dec 2003.

Volwerk, M., et al.: Compressional waves and fast flows, *Cluster Tail Workshop*, Graz, Mar 2003.

Volwerk, M., et al.: Serpentine motion oscillation of the current sheet, *Cluster Tail Workshop*, Graz, Mar 2003.

Volwerk, M., et al.: Turbulence in the Earth's magnetotail, *STAMMS Conference*, Orléans, May 2003.

Volwerk, M.: Europa's interaction with Jupiter's magnetosphere, Universität Köln, Nov 2003.

Vörös, Z., et al.: Multi-scale magnetic field intermittence, *Cluster Tail Workshop*, Graz, Mar 2003.

Vörös, Z., et al.: Multi-point statistical analysis of magnetic turbulence in the plasma sheet, *Magnetospheric Response to Solar Activity*, Prague, Sep 2003.

Vörös, Z., et al.: Turbulence spectra in the plasma sheet, *EGS-AGU-EUG Joint Assembly*, Nice, Apr 2003.

Zhang, T.L., et al.: A statistical survey of the neutral sheet, *Cluster Tail Workshop*, Graz, Mar 2003.

6.7 Posters

Badura, T., et al.: Non-Conservative Forces in the context of the Energy Integral for Gravity Field Analyses with GOCE SST Data, *Geodätische Woche*, Hamburg, Sep 2003.

Boudjada, M.Y., A. Stangl, S. Sawas, V.V. Zaitsev, H.O. Rucker, W. Voller: Remote sensing of the Solar Corona using Decametric Solar bursts, *EGS-AGU-EUG Joint Assembly*, Nice, Apr 2003.

Boudjada, M.Y., et al.: Unusual micro-structures observed during solar decametric storms, *EGS-AGU-EUG Joint Assembly*, Nice, Apr 2003.

Boudjada, M.Y.: Instrumental polarization aspects to investigate radio wave modes, *EGS-AGU-EUG Joint Assembly*, Nice, Apr 2003.

Fischer, G., W. Macher, H.O. Rucker and the Cassini/RPWS team: Reception properties of the Cassini/RPWS antennas from 1 to 16 MHz, *EGS-AGU-EUG Joint Assembly*, Nice, Apr 2003.

Kargl et al., G.: Soil strength measurements in martian analog material, *EGS-AGU-EUG Joint Assembly*, Nice, Apr 2003.

Kaufmann, E., et al.: The solid state greenhouse effect: experimental and theoretical investigation, *EGS-AGU-EUG Joint Assembly*, Nice, Apr 2003.

Khodachenko, M.L., H. O. Rucker: Electromagnetic inductive models for the loop-loop flaring interaction, *EGS-AGU-EUG Joint Assembly*, Nice, Apr 2003.

Khodachenko, M.L., H.O. Rucker: Inductive interaction of coronal currents as a possible source for magnetic loops oscillations in solar active regions, *SOHO13*, Palma de Mallorca, Sep 2003.

Khodachenko, M.L., H.O. Rucker: Inductive models of the loop-loop flaring interaction, *EGS-AGU-EUG Joint Assembly*, Nice, Apr 2003.

Khodachenko, M.L., T.D. Arber, H.O. Rucker: Collisional and viscous damping of MHD waves in partially ionized solar plasmas, *SOHO13*, Palma de Mallorca, Sep 2003.

Kolb, C., et al.: Simulation of the UV-Irradiation at the Martian Surface for Exobiology Experiments, *3rd European Workshop on Exo/Astrobiology*, Madrid, Nov 2003.

Kolb, C., R. Abart, E. Wappis, T. Penz, E.K. Jessberger, H. Lammer: The Meteoritic Component on the Surface of Mars: Implications for Organic and Inorganic Geochemistry, *Meeting of the Meteoritical Society*, Münster, Jul 2003.

Kolb, C., R. Abart, E. Wappis, T. Penz, H. Lammer, E.K. Jessberger: The Meteoritic Input on Mars - Influence on Organic Geochemistry, *3rd European Workshop on Exo/Astrobiology*, Madrid, Nov 2003.

Kolb, C., R. Abart, G. Raggl, P. Ulmer, W. Lottermoser: Synthetic Mars Analogue Materials, *MinPet*, Neukirchen, Sep 2003.

Kolb, C., R. Abart, H. Lammer: Regolith Mixing Relationships on the Surface of Mars: Implications for the Oxygen Content of the Martian atmosphere, *National Symp. on Swiss Geosciences*, Basel, Nov 2003.

Lammer, H., F. Selsis, I. Ribas, E.F. Guinan, W.W. Weiss, S.J. Bauer: Hydrodynamic escape of exoplanetary atmospheres, *2nd Eddington Workshop*, Palermo, Apr 2003.

Lammer, H., F. Selsis, I. Ribas, W.W. Weiss, S.J. Bauer: Migrating Neptune-like planets as a source of large terrestrial planets, *Toward other Earths*, Heidelberg, Apr 2003.

Lammer, H., G. Povoden, F. Selsis, I. Ribas, M.G. Tehrany, E.F. Guinan, A. Hanslmeier, S.J. Bauer: Evolution of Titan's atmosphere, *EGS-AGU-EUG Joint Assembly*, Nice, Apr 2003.

Lammer, H., et al.: Mercury's solar wind interaction during the evolution of the solar radiation and particle environment, *EGS-AGU-EUG Joint Assembly*, Nice, Apr 2003.

Lammer, H., R. Dvorak, E. Pilat-Lohinger, I. Ribas, F. Selsis, E.F. Guinan, W.W. Weiss, S.J. Bauer: Atmosphere and orbital stability of exosolar planets orbiting gamma Cephei, *EGS-AGU-EUG Joint Assembly*, Nice, Apr 2003.

Leubner, M.P.: Variation of solar wind ion distribution characteristics over shock transition layers, *EGS-AGU-EUG Joint Assembly*, Nice, Apr 2003.

Lichtenegger, H.I.M., H. Lammer, C. Kolb, T. Penz, U.V. Amerstorfer, H.K. Biernat, T.L. Zhang, W. Baumjohann: Thermal and non-thermal Escape of Hydrogen and Oxygen at Venus, *EGS-AGU-EUG Joint Assembly*, Nice, Apr 2003.

Metzler, B.: Regularization of GOCE Normal Equations, *Geodät. Woche*, Hamburg, Sep 2003.

Nakamura, R., et al.: Flow shear near the boundary of the plasma sheet during substorm expansion observed by Cluster and Geotail, *EGS-AGU-EUG Joint Assembly*, Nice, Apr 2003.

Ottacher, H., M.B. Steller, J. Heihsler: COROT - BEX an example of fast data separation, *Winter School of Astrophysics*, Tenerife, Nov 2003.

Pesec, P., E. Cristea, W. Hausleitner: Altimeter calibration with a dedicated transponder, *EGS-AGU-EUG Joint Assembly*, Nice, Apr 2003.

Rucker, H.O., U. Taubenschuss, M. Leitner, A. Lecacheux, A.A. Konovalenko, M.Y. Boudjada, R. Leitinger: Simultaneous decameter radio observations, *EGS-AGU-EUG Joint Assembly*, Nice, Apr 2003.

Runov, A.V., et al.: Current sheet bifurcations observed by Cluster during plasma sheet flap-

ping, *EGS-AGU-EUG Joint Assembly*, Nice, Apr 2003.

Vogl, D.F., et al.: Plasma and field parameters across the bow shock of Jupiter - type exoplanets in the vicinity of their host stars, *5th COROT Week*, Berlin, Dec 2003.

Volwerk, M., et al.: Fast flows and compressional waves in the magnetotail, *IUGG Assembly*, Sapporo, Jul 2003.

Volwerk, M., et al.: Fast Flows and Compressional Waves in the Earth's Magnetotail, *EGS-AGU-EUG Joint Assembly*, Nice, Apr 2003.

Vörös, Z., et al.: Multipoint analysis of magnetic turbulence in the plasma sheet, *IUGG Assembly*, Sapporo, Jul 2003.

Vörös, Z., et al.: Multifractal and wavelet analysis of magnetic turbulence in the plasma sheet, *EGS-AGU-EUG Joint Assembly*, Nice, Apr 2003.

6.8 Co-Authored Presentations

Abart, R., C. Kolb: The use of Photo Electron Spectroscopy in Mars Surface Science, Institute for Physics, University of Basel, Mar 2003.

Amerstorfer, U.V., H. Lammer, T. Tokano, F. Selsis, C. Kolb, A. Bérces, G. Kovács, M.R. Patel, C.S. Cockell, Gy. Rontó, T. Penz, N. Erkaev, H.K. Biernat: Evolution of the Martian surface pressure: Implications for the surface environment, *3rd European Workshop on Exo/Astrobiology*, Madrid, Nov 2003.

Bérces, A., H. Lammer, G. Kovács, Gy. Rontó, G. Kargl, N.I. Kömle, S.J. Bauer: Life and the solar UV environment on early Earth, *EGS-AGU-EUG Joint Assembly*, Nice, Apr 2003.

Cecconi, B., D.F. Vogl, P. Zarka, W.S. Kurth, D. Gurnett: Calibration of the Cassini RPWS antenna system through analytical inversion, *EGS-AGU-EUG Joint Assembly*, Nice, Apr 2003.

Gubchenko, V.N., V.V. Zaitsev, H.K. Biernat, M.L. Khodachenko, H.O. Rucker: Plasma kinetic models of a 3D solar corona and heliosphere, *1st Central European Solar Physics Meeting*, Bairisch Kölldorf, Oct 2003.

Hamal, K., I. Prochazka, J. Blazej, G. Kirchner, U. Schreiebr, S. Riepl, P. Sperber, W. Gurtner, et al.: Satellite Laser Ranging Portable Calibration Standard Missions 1997-2002, *EGS-AGU-EUG Joint Assembly*, Nice, Apr 2003.

Hyden, W., W. Macher, G. Kargl, C. Kolb, H. Lammer, H.O. Rucker: Implications of dielectric properties of the Martian surface soil on the search for subsurface liquid water or ice reservoirs, *3rd European Workshop on Exo/Astrobiology*, Madrid, Nov 2003.

Jankovicova, D., Z. Vörös: Multi-scale and regularity/irregularity aspects of magnetospheric dynamics, *EGS-AGU-EUG Joint Assembly*, Nice, Apr 2003.

Jankvicova, D. and Vörös, Z.: Multi-scale and regularity/irregularity aspects of magnetospheric dynamics in artificial neural networks, *Magnetospheric Response to Solar Activity*, Prague, Sep 2003.

Jaritz, G.F., R.A. Treumann, D.F. Vogl, H.K. Biernat: Analysis of a parallel fast shock and its environment for anisotropic plasma conditions, *EGS-AGU-EUG Joint Assembly*, Nice, Apr 2003.

Konovalenko, A.A., I.S. Falkovich, A.A. Gridin, A. Lecacheux, C. Rosolen, H.O. Rucker: Some requirements for the future giant low frequency ground-based radio telescopes, *EGS-AGU-EUG Joint Assembly*, Nice, Apr 2003.

Konovalenko, A.A., I.S. Falkovich, N.N. Kalinichenko, M.R. Olyak, I.N. Bubnov, A. Lecacheux, C. Rosolen, J.-L. Bougeret, H.O. Rucker, R. Leitinger: The using of large ground-based low frequency radio telescopes for outer solar corona diagnostics, *EGS-AGU-EUG Joint Assembly*, Nice, Apr 2003.

Lecacheux, A., A.A. Konovalenko, H.O. Rucker: Using large radio telescopes at decametre wavelengths, *EGS-AGU-EUG Joint Assembly*, Nice, Apr 2003.

Litvinenko, G., V. Vinogradov, H.O. Rucker, M. Leitner, V. Shaposhnikov: Complex analysis of Jovian S-bursts internal structure, *EGS-AGU-EUG Joint Assembly*, Nice, Apr 2003.

Massetti, S., S. Orsini, H. Lammer, A. Mura, P. Wurz, A. Milillo, A.M. Di Lellis, E. De Angelis: Dynamics of the solar wind-induced cusp-associated sputtering emission from the surface of Mercury, *EGS-AGU-EUG Joint Assembly*, Nice, Apr 2003.

Matsuoka, A., W. Baumjohann: The magnetic field experiment for BepiColombo MMO, *IUGG Assembly*, Sapporo, Jul 2003.

Matsuoka, A., W. Baumjohann: The magnetic field experiment for BepiColombo MMO, 2, *EGS-AGU-EUG Joint Assembly*, Nice, Apr 2003.

Melnik, V.N., A.A. Konovalenko, A.A. Stanislavskii, E.P. Abranin, V.V. Dorovskii, V. V. Zaharenko, V. N. Lisachenko, H.O. Rucker, M.Y. Boudjada, A. Lecacheux, C. Rosolen: Observations of solar Type II bursts at decameter wavelengths, *EGS-AGU-EUG Joint Assembly*, Nice, Apr 2003.

Molina-Cuberos, G.J., J.A. Morente, J. Porti, A. Salinas, K. Schwingenschuh, H.I.M. Lichtenegger, B.P. Besser, H.U. Eichelberger, J. Margineda: Schumann resonances on Mars: Numerical simulations, *EGS-AGU-EUG Joint Assembly*, Nice, Apr 2003.

Motschmann, U., J.M. Grießmeier, K.H. Glaßmeier, E. Kührt, H.O. Rucker: Erzeugung von Radiostrahlung in Exomagnetosphären, *Planetenbildung: Das Sonnensystem und extrasolare Planeten*, Weimar, Feb 2003.

Penz, T., A. Stadelmann, H. Lammer, J.-M. Grießmeier, F. Selsis, H.K. Biernat, A. Hanslmeier: The influence of the interior structure of Uranus-type extrasolar planets on their stellar wind interaction, *5th COROT Week*, Berlin, Dec 2003.

Penz, T., H. Lammer, H.K. Biernat, N.V. Erkaev, H. Gunell, E. Kallio, M. Holmström, S. Barabash, T.L. Zhang, H.I.M. Lichtenegger, W. Baumjohann: Atmospheric loss caused by Kelvin-Helmholtz instability: What can we expect from Mars- and Venus Express? *EGS-AGU-EUG Joint Assembly*, Nice, Apr 2003.

Penz, T., H.K. Biernat, V.S. Semenov: Remote sensing of reconnection structures, *26th Ann. Seminar*, Apatity, Feb 2003.

Penz, T., J.-M. Griessmeier, A. Stadelmann, H.I.M. Lichtenegger, H. Lammer, F. Selsis, I. Ribas, H.K. Biernat, W.W. Weiss: Magnetosphere-stellar wind interaction of „Hot Jupiters", *4th COROT Week*, Marseille, Jun 2003.

Pérez-Ayúcar, M., O. Witasse, J.-P. Lebreton, B. Kazeminejad, D.H. Atkinson: A Simulated Dataset of the Huygens Mission, *Int. Workshop on Planetary Probe Atmospheric Entry and Descent Trajectory Analysis and Science*, Lisbon, Oct 2003.

Petrukovich, A.A., W. Baumjohann, R. Nakamura, A. Balogh, K.-H. Glaßmeier: Vertical current sheets in the magnetotail under northward IMF, *EGS-AGU-EUG Joint Assembly*, Nice, Apr 2003.

Sacher, S., C. Kolb, G. Krammer, H. Lammer, G. Kargl, C.S. Cockell, A. Bérces, R. Abart: Simulation of the Martian Atmosphere for Exobiology Experiments with Special Emphasis on the Water Content, *3rd European Workshop on Exo/Astrobiology*, Madrid, Nov 2003.

Vellante, M., H. Luehr, T.L. Zhang, U. Villante, M. De Lauretis, A. Piancatelli, M. Rother, K. Schwingenschuh, W. Koren, W. Magnes: A comparative study of geomagnetic pulsations simultaneously observed on space by champ satellite and at ground by the segma magnetometer array, *EGS-AGU-EUG Joint Assembly*, Nice, Apr 2003.

Veselov, M.V., K.M. Torkar, N.Yu. Buzulukova: Plasma density determination along a high elliptic orbit, *EGS-AGU-EUG Joint Assembly*, Nice, Apr 2003.

Veselov, M.V., L.V. Zinin, N.Yu. Buzulukova, D.V. Chugunin, V.E. Kunitsyn, I.V. Silin, K.M. Torkar: Thermal plasma density measurements from a positively charged spacecraft: overview of the last decade and perspectives, *Auroral Phenomena and Solar-Terrestrial Relations*, Moscow, Feb 2003.

Villante, U., M. Piersanti, P. Di Giuseppe, M. Vellante, T.L. Zhang, W. Magnes: The SSC event of April 17 2002: a preliminary analysis from SEGMA array, *Workshops on Sun-Earth connection space weather during April 14-24, 2002 storms*, Laurel, Aug 2003.

Zaitsev, V.V., V.E. Shaposhnikov, H.O. Rucker: Electron acceleration in the ionosphere of Io, *Actual problems of physics of solar and stellar activity*, Nizhny Novgorod, Jun 2003.

Zaitsev, V.V., V.E. Shaposhnikov, H.O. Rucker: Escaping of electron cyclotron maser emission from the hot stellar corona, *Actual problems of physics of solar and stellar activity*, Nizhny Novgorod, Jun 2003.

7 Teaching & Workshops

7.1 Lecturing

IWF members are actively engaged in teaching at three universities. In summer 2003 and in the current winter term 2003/2004 the following lectures are given, in addition to a number of practical exercises and seminars. The majority of the lectures are given in German.

KFU Graz

Hydrodynamics (Biernat)

Plasmaphysics (Biernat)

Two-component Magnetohydrodynamics (Selected Chapters of Space Physics and Aeronomy) (Biernat)

Solar-Terrestrial Relations (incl. Space Weather) (Biernat)

Ice and Fire in the Solar System: Comets, Moons, and Planets (Selected Chapters of Classical Geophysics) (Kömle/Lammer)

Methods of Data Analysis and Inversion (Rucker)

Planing, Organisation, and Management of Geophysical Projects (Mühlbachler, Rucker)

Magnetospheres of Planets (Rucker)

Introduction to Plasma Physics (Selected Chapters of Space Physics and Aeronomy) (Rucker)

TU Graz

Satellite Geodesy (Sünkel)

Signal Processor Techniques (Magnes)

Investigation of Planetary and Interplanetary Magnetic Fields (Schwingenschuh)

Space-Time Reference Systems (Sünkel)

HF-Engineering 1+2 (Riedler)

JKU Linz

Mathematics for Students of Computer Sciences in Economics I+II (Hausleitner)

Advanced Course

The joint two-years post-graduate university course MAS Space Sciences at both Karl-Franzens University of Graz and Graz University of Technology terminated in summer 2003 with the fourth semester and several candidates finished their master theses and defensio. Several members of IWF supervised these master theses.

In fall 2003 a new two-years post-graduate university course MSc Space Sciences started (www.spacesciences.oeaw.ac.at), leading to the international acknowledged Master of Science. Again several members of IWF are lecturers of this inter-university course led by H.O. Rucker.

7.2 Habilitations

Kömle, N.I.: Cometary surface processes: Experiments and theory, Habilitation, KFU Graz, 34 pages (2003)

7.3 Theses

Besides lecturing, members of the Institute are supervising Diploma and Doctoral Theses. In 2003, the following theses have been completed:

Bodiselitsch, B.: The Martian meteorites: the key to explaining the evolution of the Martian atmosphere? Master Thesis, University Course MAS

Space Sciences (Supervisors: H. Lammer/H.O. Rucker)

Feldhofer, H.: Advanced magnetic field cleanliness techniques for space missions with magnetic field experiments, Doctoral Thesis, TU Graz (Supervisors: W. Riedler, H.K. Biernat, M. Delva)

Jaritz, G.F.: Anisotropic fast shocks: Application to the Earth's bow shock, Diploma Thesis, KFU Graz (Supervisors: H.K. Biernat, D.F. Vogl)

Langmayr, D.: Energy transport along magnetic flux tubes and application to the Io-Jupiter interaction, Doctoral Thesis, KFU Graz (Supervisors: H.O. Rucker, H.K. Biernat)

Leitner, Martin: The sheath region of interplanetary magnetic clouds modelled as force-free cylindrical magnetic flux ropes: HELIOS and WIND observations, Diploma Thesis, KFU Graz (Supervisor: H.K. Biernat)

Leitner, Michael: A guide through waveform analysis: From instrumentation to data analysis and data interpretation, University Course MAS Space Sciences (Supervisor: H.O. Rucker)

Penz, T.: Magnetohydrodynamic instabilities at the ionopause of Venus and Mars and their influence on atmospheric ion loss, Diploma Thesis, KFU Graz (Supervisors: H.K. Biernat, H. Lammer)

Steiner, R.: Novel procedures for modelling the high-latitude ionosphere, Doctoral Thesis, TU Graz (Supervisors: M. Friedrich, K. Torkar)

Taubenschuß, U.: Simultaneous ground-based and spacecraft observations of Jovian radio emission, Diploma Thesis, KFU Graz (Supervisor: H.O. Rucker)

7.4 Science Meetings

From March 26-28, 2003 the IWF hosted the *Cluster* Tail Workshop, which was organized by R. Nakamura and W. Baumjohann. More than 50 participants from 14 nations have attended this workshop. See http://cluster-tailworkshop-graz.oeaw.ac.at for details.

In addition, W. Baumjohann and H.O. Rucker each organized a session at the EGS-AGU-EUG Joint Assembly in Nice, France.

7.5 Project Meetings

In 2003 several project meetings were organized at IWF, two of them with international participation.

From February 5-7, 2003, the System Specification Review for the Ground Data System of the *Double Star* Project was held at IWF. 21 participants from 6 countries including 8 participants from the P. R. China provided the basis for the implementation of the data system.

The 8th *Huygens* Descent Trajectory Working Group (DTWG) and the 24th Science Working Team Meeting (HSWT) was hosted by IWF from September 30 to October 3, 2003. About 56 participants from 8 different countries have attended this workshop.

8 Personnel

Arsov, Kirčo, Dr. (S)
Asano Yoshihiro, Dr. (E, ESA)
Aydogar, Özer, Mag. Dipl.-Ing. (E)
Badura, Thomas, Dipl.-Ing. (S, RFTE/ASAP)
Baumjohann, Wolfgang, Prof. (E)
Berghofer, Gerhard, Ing. (E)
Besser, Bruno P., Dr. (E)
Biernat, Helfried K., Prof. (P)
Boudjada Mohammed Y., Dr. (P)
Chwoika, Rudolf (S)
Cristea, Elena, Dipl.-Ing. (S, part. UN)
Delva, Magda, Dr. (E)
Eichelberger, Hans U., Dipl.-Ing. (E, BMVIT)
Fischer, Georg, Dipl.-Ing. (P)
Flock, Barbara, Mag. (E)
Fremuth, Gerhard, Dipl.-Ing. (E)
Giner, Franz, Dipl.-Ing. (E)
Graf, Christian, Ing. (S)
Hausleitner, Walter, Dr. (S)
Heihsler, Johann, Dipl.-Ing. (E, BMBWK)
Höck, Eduard, Dipl.-Ing. (S)
Jernej, Irmgard, Ing. (E)
Jeszenszky, Harald, Dipl.-Ing. (E)
Jetzl, Ilse, Dr. (P)
Kargl, Günter, Dr. (P)
Kaufmann, Erika, Mag. (P, FWF)
Kazeminejad, Bobby, Dipl.-Ing. (P, ESA)
Khodachenko, Maxim L., Dr. (P)
Kirchner, Georg, Dr. (S)
Kögler, Gerald (I)
Koidl, Franz, Ing. (S)
Kolb, Christoph, Mag. (P)
Kömle, Norbert I., Univ.-Doz. (P)
Koren, Wolfgang, Ing. (E)
Kürbisch, Christoph, Ing. (E)
Laky, Gunter, Dipl.-Ing. (E)
Lammer, Helmut, Dr. (P)
Leubner, Manfred P., Dr. (P, BMBWK)
Lichtenegger, Herbert I.M., Dr. (E)
Macher, Wolfgang, Dipl.-Ing. (P)
Magnes, Werner, Dr. (E)
Metzler, Bernhard, Dipl.-Ing. (S, RFTE/ASAP)
Močnik, Karl, Dr. (E)
Mühlbachler, Stefan, Dr. (P, RFTE)
Nakamura, Rumi, Dr. (P)
Neukirchner, Sonja, Ing. (E)
Ottacher, Harald, Mag. (E, BMBWK & ESA)
Pešec, Peter, Dr. (S)
Preimesberger, Thomas, Dipl.-Ing. (S, RFTE/ASAP)
Riedler, Willibald, Prof. em. (E, BMBWK)
Rucker, Helmut O., Prof. (P)
Runov, Andrei V., Dr. (E)
Scherr, Alexandra, Mag. (I)
Schwingenschuh, Konrad, Dr. (E)
Slamanig, Herwig, Dipl.-Ing. (I, BMBWK)
Stachel, Manfred, Ing. (E, ESA)
Stangl, Günter, Dipl.-Ing. (S, BEV)
Steller, Manfred B., Dr. (E)
Stieninger, Reinhard, Ing. (S, Stmk.)
Stock, Daniel (E)
Sucker, Michael, Dipl.-Ing. (S)
Sünkel, Hans, Prof. (S, BMBWK)
Taubenschuss, Ulrich, Mag. (P, FWF)
Torkar, Klaus M., Univ.-Doz. (E)
Valavanoglou, Aris, Dipl.-Ing. (E)
Vogl, Dieter F., Dr. (P)
Voller, Wolfgang G., Mag. (P)
Volwerk, Martin, Dr. (E, MPE)
Vörös, Zoltán, Dr. (E)
Wallner, Robert, Ing. (E)
Zambelli, Werner (E, part. RFTE)
Zehetleitner, Sigrid (S & I)
Zhang, Tie-Long, Dr. (E)
Zöhrer, Alexander, Dipl.-Ing. (P, ASAP)

As of December 31, 2003

E: Experimental Space Research, P: Extraterrestrial Physics, S: Satellite Geodesy, I: Institute Administration. Most positions are directly funded through ÖAW, others as indicated by: ASAP: Austrian Space Applications Programme, BEV: Federal Office for Metrology and Surveying, BMBWK: Federal Ministry for Education, Science and Culture, BMVIT: Federal Ministry of Transport, Innovation and Technology, ESA: European Space Agency, FWF: Austrian Science Fund, MPE: Max-Planck Institute for Extraterrestrial Physics, RFTE: Austrian Council for Research and Technology Development, Stmk.: State of Styria, UN: United Nations.